Statistical analysis of seasonal rainfall variability in Ethiopia and its teleconnection with global sea surface temperatures

[エチオピアにおける降水量の季節変動の統計的解析と全球海面水温 とのテレコネクション]

Asmaa Abdallah Talkhan Alhamshry

Tottori University, Japan

2020

Statistical analysis of seasonal rainfall variability in Ethiopia and its teleconnection with global sea surface temperatures

[エチオピアにおける降水量の季節変動の統計的解析
と全球海面水温とのテレコネクション]

By

Asmaa Abdallah Talkhan Alhamshry

A thesis submitted to the United Graduate School of Agricultural Sciences, Tottori University in partial fulfillment of the requirements for the degree of Doctor of Philosophy in Global Arid Land Science

Major Supervisor:

Katsuyuki Shimizu (Prof.)

Co–supervisors:

Yasuomi Ibaraki (Prof.)

Kimura Reiji (Assoc. Prof.)

DEDICATION

To my soulmate!!

Acknowledgements

First and foremost, I would like to thank the Almighty Allah (my God) for his mercy and showers of blessings all the way throughout my life. I praise Allah for giving me strength, good health, knowledge and wisdom to successfully complete my PhD research.

I am deeply indebted to the Government of Egypt (Cultural Affairs and Missions Sector) for providing this study opportunity and financial support through Egypt-Japan Education Partnership (EJEP) scholarship and the National Research Centre (NRC) for granting me a study leave.

This research would not have been possible without the very helpful individuals around me. It is a great pleasure for me to acknowledge those who contributed to the success of my PhD study.

First, I would like to express my deep and sincere gratitude to my major supervisor Prof. Katsuyuki Shimizu for his great support, invaluable and constructive advice, and encouragement during my PhD research. I also thank my co-supervisors Prof. Yasuomi Ibaraki and Assoc. Prof. Kimura Reiji for their helpful comments and suggestions. My sincere thanks with high appreciation go to Prof. Hiroshi Yasuda and Assoc. Prof. Ayele Almaw Fenta who provided myriad useful comments and guidance to make this PhD study come to fruition. I'm also grateful to all members of Environmental Conservation Division (Hydrology subdivision), especially Dr. Takayuki Kawai and Eiji Seki (M.Sc. student) for their unreserved support.

I would also like to extend my thanks for all members of Water Use and Management Lab (Uchida-san, Freeg-san, Ryoma-san, and Moeka-san) for their support during my study and my daily life in Japan. Special thanks to my friends Hassan Mohamed, Tamara Sideeq, and Imad Al-Taweel for their kind help and support.

I also thank all administrative staff members of Tottori University who have always been willing to provide support and administrative information, especially Taniguchi-san and Midori-san.

I would like to extend my appreciation to Prof. Hany El-Nazer, the former president of the National Research Centre in Egypt who believes in the power of young researchers and to Dr. Abd El-Ahd Gamal El-Din who wished to see my dream come true, but left early!!

Most importantly, I would like to forward my special thanks to Dr. Mostafa Abu-Bakr and Dr. Ahmed Gaber for their unwavering support and encouragement. I offer my warmest thanks for Prof. Hesham El-Kaliouby, head of Geophysics Department, for his unreserved support and for all my colleagues at Geophysics Department, National Research Centre, Egypt.

I am also grateful to my family and friends, especially Dr. Amany Gaballa and Dr. Mona Mohamed back home for their gracious support and prayers throughout the years.

Last but not least, I extend my heartily appreciation to the whole people of Japan, especially people of Tottori Prefecture for making me feel home away from my home, especially Akiko Sawada-san.

Table of Contents

List of Figures

List of Tables

List of Abbreviations

ANN	Artificial Neural Network
AO	Arctic Oscillation
CGIAR	Consultative Group for International Agricultural Research
CHIRPS	Climate Hazards Infra-Red Precipitation with Stations
CRU	Climate Research Unit
CSI	Consortium for Spatial Information
CV	Coefficients of Variation
DEM	Digital Elevation Model
EEPCo	Ethiopian Electric and Power Corporation
ETM+	Enhanced Thematic Mapper plus
ENSO	El Niño–Southern Oscillation
FMAM	February March April May
FAO	Food and Agriculture Organization
GSST	Global Sea Surface Temperature
HadISST	Hadley Sea ice and Sea surface Temperature
IOD	Indian Ocean Dipole
ITCZ	Intertropical Convergence Zone
JJAS	June July August September
MoFED	Ministry of Finance and Economic development
MOI	Mediterranean Oscillation Index
NAO	North Atlantic Oscillation
NASA	National Aeronautics and Space Administration
NMA	National Mapping Agency
NMA	National Meteorology Agency

ONDJ	October November December January
PDO	Pacific Decadal Oscillation
SRTM	Shuttle Radar Topography Mission
SOI	Southern Oscillation Index
SON	September October November
SST	Sea Surface Temperature
SSTs	Sea Surface Temperatures
UNESCO	United Nations Educational, Scientific, and Cultural Organization
UBNB	Upper Blue Nile Basin

Chapter 1

General introduction

1.1. Background

1.1.1. Topography and river basins of Ethiopia

Ethiopia is considered as one of the largest countries in the continent of Africa with an entire area of about 1.13×10^6 km^2 extending from latitude 3° to 15° N and longitude 33° to 48° E. The country is characterized by high complex of topography with high and lowlands, where the remarkable variations in elevation ranges from hundreds of meters below sea level at the northeastern areas to thousands of meters above sea level at the highlands of the northern parts.

Ethiopia as one of the east African countries was affected by the Great Rift Valley that separated the country into two main plateaus (southeastern and western highlands) causing a high terrain complexity due to its extension from northeast to southwest of the country (Figure 1.1). The rift system has two flanks surrounded by southeastern highlands to the eastern flank and to the western flank are the western highlands with massive mountain ranges divided by steep and deep sided valleys of the main rivers, while the lowlands are located to the south and east of the southeastern highlands and to the west side of the western highlands.

On one hand, the country is distinguished by an essential amount of water resources and the majority of its river basins are derived from the high mountain ranges and are accelerated across systems of steep valley. On the other hand, the hydrological setting is highly variable in the region. As shown in (Figure 1.1), Ethiopia has twelve basins as following: (i) eight river basins; (ii) one lake basin (Lake Tana basin); (iii) the three other basins are dry.

In 2016, the Food and Agriculture Organization (FAO) detected the river basins from the three main drainage systems as follows;

1. The Nile basin including Blue Nile or Abbay, Tekeze and Mereb, and Baro-Akobo basins. Abtew and Melesse in 2014 investigated that the Nile Basin contributes about 85% of the Nile river annual flow and it covers about 33% of Ethiopia and it drains the northern and central regions westwards.
2. The Rift Valley basin including Danakil, Awash, Central Lakes, and Omo-Gibe basins. It represents about 28% of the Ethiopian area with a set of separate interior basins expanded from Djibouti in the north to the United Republic of Tanzania in the south, where about 50% of its total area is located in Ethiopia.
3. The South-East basin including Ogaden, Genale-Dawa, Wabi-Shebelle basins. About 39% of the country is covered by this basin and it drains the southeastern mountains towards the Indian Ocean and the Republic of Somalia.

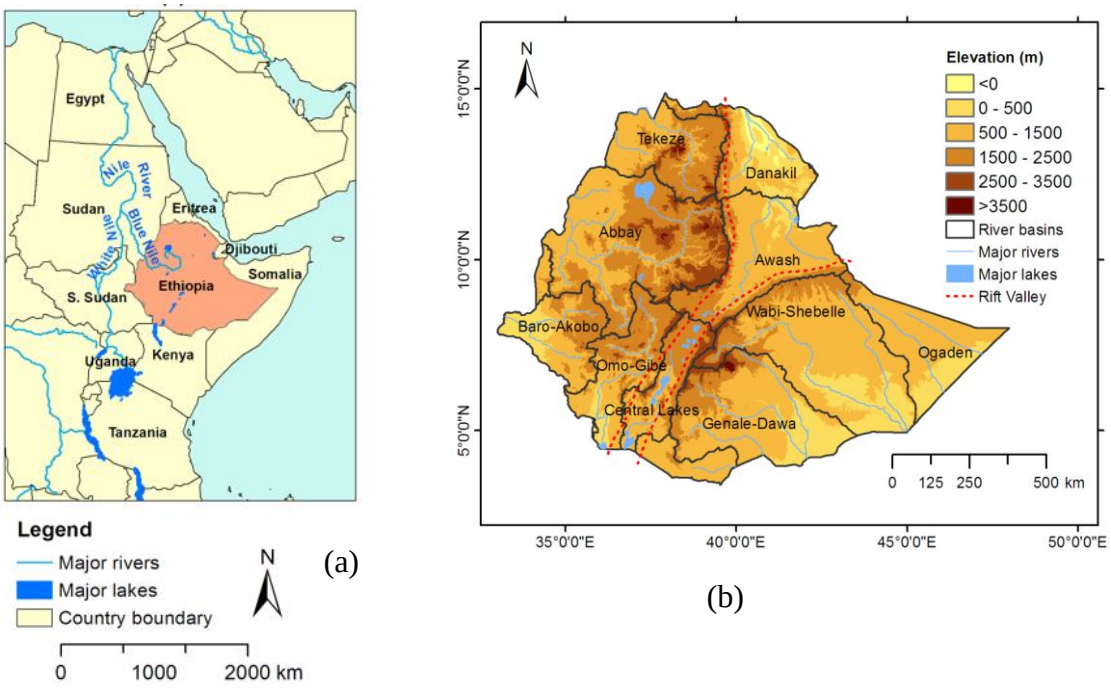

Figure 1.1 (a) Location map of Ethiopia and (b) Topography and Ethiopian main river basins of extracted from Shuttle Radar Topography Mission (SRTM) with 90 m resolution and Digital Elevation Model (DEM) (map (b) is after Fenta 2018).

The river basins originated from the western highlands flow towards the west into the basin system of the Nile River, the latter is passing through Sudan and Egypt and those derived from the eastern highlands flow easterly into the Republic of Somalia. The estimated potential of Ethiopian surface water of about 120 billion m^3/year is derived from these twelve river basins. The majority (about 80%) of surface water, originating from the western and southeastern highlands with high rainfall amounts, is lost as runoff to the neighbor countries (FAO 2016). Thus, Ethiopia represents the water tower for the Horn of Africa.

The Ethiopian groundwater resources is low compared to the resources of surface water and its potentiality was estimated of about 2.6 billion m^3/year. Thus, the country has the ability to irrigate about 5 million ha depending on these existing resources of water (Awlachew 2010). Furthermore, the MoFED in 2010 estimated the potential of the country's hydropower of about 45,000 MW. Nevertheless, such high potentials are not fully invested because of some technical challenges, limited resources of finance, and lack of decision makers in the government who have a perfect plan for utilizing these potentials (Berhaun et al. 2014). Consequently, Ethiopia has some obstacles to meet the increased demand for water supply, food, and energy because of the increasing rate of population, urbanization's rapid expansion and various economic activities.

1.1.2. Climate of Ethiopia

Given the Ethiopian high variability of topography and the geographic location close to the Indian Ocean and the equator, the spatial and temporal variations in precipitation (mainly rainfall) and temperature are high over the country (Gamachu 1988; Fazini et al. 2015). The main climatological factors influencing the rainfall over the country: (i) the migration of the Intertropical Convergence Zone (ITCZ) seasonally (Beltrando and Camberlin 1993); (ii) warm lows formed

over the Arabian landmasses and Sahara; (iii) formation of sub-tropical high pressure over the Azores; (iv) flow of cross-equatorial moisture from the southern, central, and equatorial parts of the Indian Ocean, tropical Africa, and Atlantic Ocean, respectively; (v) flow of the upper-level tropical easterly jet over Ethiopia; and (vi) low-level Somali jet (Korecha and Barnston 2007). Moreover, high topographic and marked variations in altitudes over vast areas of Ethiopia and the proximity of the continent of Asia have to be considered (Berhaun et al. 2014; Fazini et al. 2015; Fenta et al. 2017a).

Climate spatial variations include the rainfall seasonal cycle, amount, onset and cessation times, and length of growing season (Gamachu 1988; Segele and Lamb 2005). Sometimes rainfall can be temporally varied from days to decades in terms of the magnitude and direction of rainfall trends over seasons and regions (Jury and Funk 2012; Seleshi and Zanke 2004). These spatio-temporal variations in Ethiopian rainfall are attributed to the variable altitudes (Gamachu 1988). Moreover, the variable Sea Surface Temperatures (SSTs) over the Indian, Pacific, and Atlantic Oceans (Segele et al. 2009a & Segele et al. 2009b; Korecha and Barnston 2007) and the interannual and interseasonal variations in the strength of monsoon over the Arabian Peninsula (Segele and Lamb 2005; Segele et al. 2009a, b).

Korecha and Barnston in 2007 indicated that Ethiopia exhibits three cycles of seasonal rainfall: (i) summer rainy season (locally known as Kiremt), it extends from June to September (JJAS) and controlled by Guinean monsoon, of equatorial humid and warm winds, and orographic variations result in a plenty of rains; (ii) winter dry season (Bega) extending from October to January (ONDJ) and influenced by the trade winds blowing from northeast to southwest of the country. These relatively cool but rather dry winds originated from the contrast between the equatorial low pressures and the thermal anticyclone of Egypt and western Asia. (iii) spring mid-rainy season

(locally called Belg) that ranges from February to May (FMAM) and influenced by the Congo basin's southwestern winds causing relatively rains over the southern part of Ethiopia. Consequently, the annual rainfall is marked by high spatial variations due to such complex climatic dynamics, where the rainfall can range from few millimeters as in Danakil depression to over than 2,000 mm over the Ethiopian highlands.

The temperature in Ethiopia is highly affected by variations in altitudes (Fazini et al. 2015), where the mean annual temperatures range from 35°c at 155 m below sea level as in Danakil depression to less than zero degree at highlands of 4,000 m above sea level (UNESCO 2004). Given the topographic variations between highlands and lowlands, the landscapes in Ethiopia show a large-scale climatic variety from arid to humid areas, in addition to other significant microclimatic diversity over small regions because of the variable micro-relief.

The United Nations Environmental Program embraces the classification of Ethiopian climatic zones (Barrow 1992). The map of aridity index (the ratio between the mean annual precipitation to the mean annual potential evapotranspiration) is shown in (Figure 1.2) that indicates the climatic areas of Ethiopia as humid (26%), dry sub humid (13%), semiarid (34%), and arid regions (27%).

Rainfall is considered the most crucial climatic factor for rain-fed agriculture, hydropower projects, and social and economic development plans in Ethiopia (Conway et al. 2011). Across time and space, the rainfall shows high variations because of elevation variations and complex topography over the country (Gamachu 1988). On one side, many previous studies indicated that rainfall temporally changes from days to decades with the direction and magnitude of the historical rainfall trends, the latter is varying from season to season and from one area to another (Cheung et al. 2008; Jury and Funk 2012; Seleshi and Zanke 2004; Viste and Sorteberg 2013).

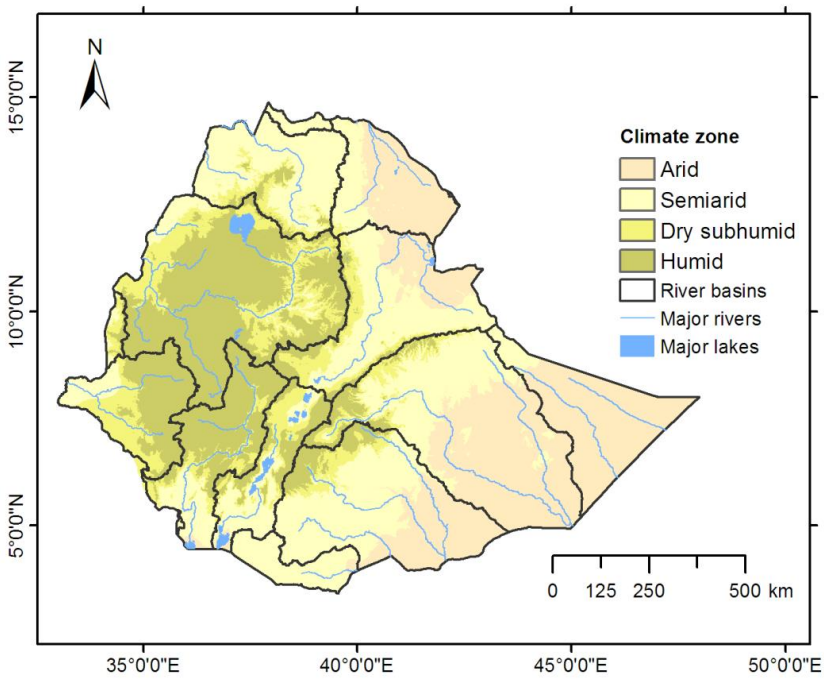

Figure 1.2 Climate classification of Ethiopia based on the Global Aridity Index dataset provided by the Consultative Group for International Agriculture Research–Consortium for Spatial Information (CGIAR-CSI) via CGIAR-CSI Geoportal (http://www.csi.cgiar.org). (After Fenta 2018).

On the other side, the rainfall is spatially variable across Ethiopia including variations in start and end times, amount, and seasonal cycle of rainfall, as well as the range of the growing season (Segele and Lamb 2005; Gamachu 1988).

These spatio-temporal rainfall variations across the country are controlled by major factors, such as variable altitudes (Gamachu 1988), the variable Sea Surface Temperatures (SSTs) over the Indian, Pacific, and Atlantic Oceans (Segele et al. 2009a, b; Korecha and Barnston 2007) and the interannual and interseasonal variations in the strength of monsoon over the Arabian Peninsula (Segele and Lamb 2005 & Segele et al. 2009a, b). Therefore, the full understating of

teleconnections or associations between SST over different oceanic regions and rainfall is crucial for producing a reliable climate prediction.

The annual north to south migration of ITCZ mainly controls the spatio-temporal variations of rainfall over Ethiopia. During summer rainy season from June to September (JJAS) (hereafter, the seasons of 4-month will be abbreviated through the first letter of every month, e.g. JJAS), the rain covers most regions of Ethiopia except southern and southeast lowlands. These rains result from the moisture fluxes coming from Atlantic and Indian Oceans due to the moving of low pressure ITCZ of the Arabian and the Sudan over Ethiopian highlands (Viste and Sorteberg 2013).

The spring season (FMAM) covers the southern, southeast, and east regions of Ethiopia. From March to May, the northward ITCZ causes the orographic rains over east-central, south-central, and southwestern parts of the country, as well as the moisture flow from Gulf of Aden and Indian Ocean, due to low pressure ITCZ over the southern part of Sudan, produces the main rainfalls at southern and south-east parts of Ethiopia, while east, north-east, and east-central regions has secondary rains (Seleshi and Zanke 2004; Viste and Sorteberg 2013; Segele et al. 2009a). In winter dry season (ONDJ), it starts with small rains from September to November covering the southern part of Ethiopia due to southward migration of ITCZ, thereafter the dry masses of air from December to February result in predominant rainfalls at southern parts of the country. These air masses are caused by either the anticyclone of Saharan and/or Arabian high-pressure ridge (Gissila et al. 2004; Kassahun 1987).

1.2. Description of the study area (Upper Blue Nile Basin)

The Upper Blue Nile Basin (UBNB), locally known as Abbay basin, occupies the western part of Ethiopian highlands with an area of about 176,000 km^2, i.e. 17% of the Ethiopian domain as

shown in (Figure 1.1). The mean annual precipitation was estimated of about 1,600 mm (Sutcliffe and Parks 1999). Moreover, about 48.5 km^3 was the estimated mean annual discharge from the basin (Conway 2000). It starts at Lake Tana with an elevation of about 1,800 m above mean sea level and ends at falls of Tississat, which vertically drop over of about 50 m (Shahin 1985).

In general, the UBNB in the western part annually receives more rainfall (1,000-2,400 mm) than other northern, eastern, and southern parts of Ethiopia. In 2010, Kloss and Legesse showed that the rainfall increases with altitude due to the orographic influence, the latter represents a prominent challenge for all prediction models of rainfall in the region. Rainfall has a crucial role in the basin hydrology, where the lack or excess of rainfall lead to undesirable droughts or flooding, respectively. Thus, it would be useful to fully investigate the rainfall forecasting models over the basin for the optimal allocation of water usage.

For Sudan and Egypt, the Nile River is considered the main water supply that comes from one of the main tributaries locating at UBNB in Ethiopia, where more than half of the total stream flow of the Nile reaches the Egyptian Aswan High Dam (Conway 2000; Seleshi and Demaree 1995; Yates and Strzepek 1998). Summer rainfall forms about 70% of the UBNB's annual rainfall (Conway 2000). Moreover, 85%-95% of agriculture in Ethiopia occurs at summer rainy season, so the UBNB is basically the most important water resource for the country and neighboring countries.

1.2.1. General overview and geology of Lake Tana basin

Lake Tana, as the largest lake in the country, is considered the main freshwater source for the Blue Nile basin (McCartney et al. 2010), as well as it is the Nile Basin's third biggest lake covering an area of about 15,000 km^2 and 15 m depth with flat bottom and the slope is steep at the borders (Alemayehu et al. 2010; Kebede et al. 2006). As shown in (Figure 1.3), it is located at the

northwestern part of Ethiopia between longitudes 36.89° and 38.25°E and latitudes 10.95° and 12.78°N, with width of 66 km and length of 84 km. It is distinguished by diverse topography with elevations ranging from (1,000-4,000 m) above mean sea level, and of about 3,156 km^2 as a surface area (Tegegne et al. 2013).

Lake Tana contains half of freshwater in Ethiopia. Only four rivers (Megech, Ribb, Gumara, and Gilgelabay) feed the lake with water, regardless of more than 40 streams and rivers flow into the lake (Alemayehu et al. 2010; Setegn et al. 2008). In 2010, Alemayehu et al. estimated the mean annual inflow of the Lake of about 158 m^3/s. The Blue Nile River represents the only surface outflow of Lake Tana with the flow of 4×10^9 m^3/year as measured at the rainfall station of Bahir Dar.

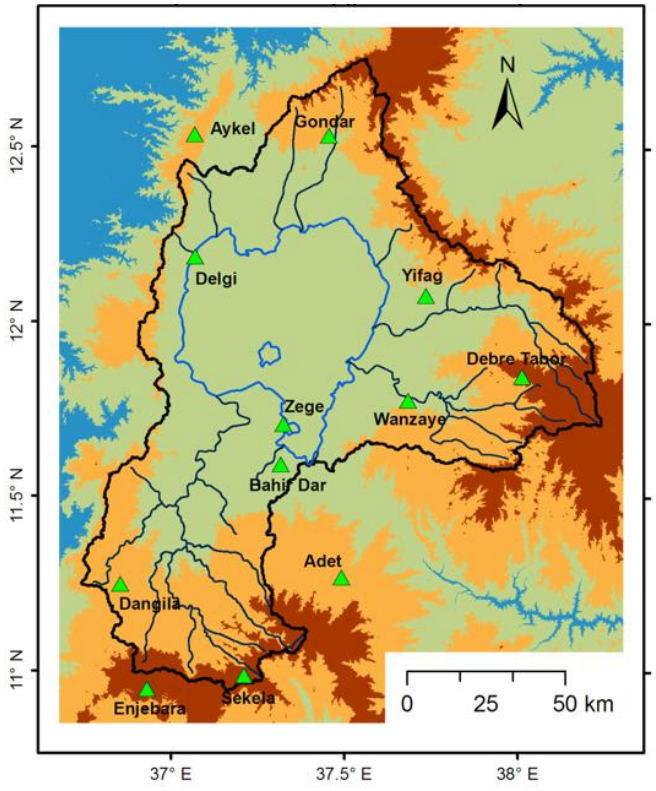

Figure 1.3 Map showing the topography of the Lake Tana basin and locations of rainfall gauging stations. Elevations are extracted from the Shuttle Radar Topographic Mission (SRTM) 30-m digital elevation model.

In early Pleistocene was the formation of Lake Tana due to the volcanic activity that blocked a number of river's course (Mohr 1962). The waterfalls were most likely created by the lava separating the headwaters of Lake Tana from the lower basin of the Blue Nile (Rzóska 1976a). A recent collection of geophysical and core data showed the accumulation of about 100 m of sediments in the lake's core (Lamb et al. 2007). In addition, the data indicated that the complete dryness of the lake occurred between 18,700 and 16,700 calibrated age BP, during the stiff deposition of the sediments at the base of lake.

From the lake's core, the periphytic diatoms and peat showed environments of shallow water and swamps of papyrus following the desiccation in the central basin between 16,700 and 15,100 calibrated age (cal) BP. The halophytic diatoms indicated the slight salinity of the lake due to the evaporation of surface water during the rise of the lake water level. At 14,750 cal BP, freshwater conditions of the lake abruptly returned, when the Lake Tana overflowed into the Blue Nile basin (Lamb et al. 2007).

1.2.2. Regime of climate over the Upper Blue Nile

The basin is mainly influenced by the migration of ITCZ that controls the amount of rainfall in the summer season. The records of rainfall indicate a high spatio-temporal variation over the UBNB locating at the western highlands of Ethiopia (Degefu 1987; Gamachu 1977; Sutcliffe and Park 1999). In 2012, Lucio et al. investigated the seasonal variability of rainfall over the basin, where the rains fall over much of the year, but the highest amount of rainfall are recorded at the wet months from July-September (JAS) due to the position of ITCZ in the northern hemisphere. Moreover, the dry season extends from November to March (NDJFM), while the transition between wet and dry seasons occurs in June and October. A little of rains fall in April and May.

Another study (Kloos and Legesse 2010) indicated that the rainy season during summer (Kiremt) at the western highlands occurs from June to September (JJAS), while the dry season (Belg) covering the northern, southern and central parts of the country occurs from February to May (FMAM). Basically, the moisture carried from the Indian Ocean by the southeasterly winds is the cause of the first rainy season over the country (FMAM), while the second season of rainfall (JJAS) is due to southeasterly and southwesterly winds. Therefore, the variations occur at the seasonal rainfall and wind could be sequenced by 3 months (OND), (JFM), (AMJ), and (JAS) or 4 months (ONDJ), (FMAM), and (JJAS).

1.3. Problem statement and objectives

Previously (Diro et al. 2011b), Ethiopia has been classified into three main subregions based on the annual cycle rainfall: (i) the southern part with two seasons of rainfall; short rains (SON) and long rains (MAM); (ii) the eastern and central parts with rainfalls recorded in summer (JJAS) and spring (FMAM); (iii) the central-western and northern parts has one season of rainfall peak recorded in July/August. Nevertheless, the seasonal rainfall over the country has a high interannual variation due to the diversities in the migration and intensity of the African ITCZ from one year to another (Segele et al. 2009a; Kassahun 1987).

The teleconnections between rainfall over Ethiopia and oceanic Sea Surface Temperatures (SSTs) plays a crucial role for enhancing the forecasting models of rainfall over the country, so this relation needs to be fully understood. However, these teleconnections between SSTs and variations in rainfall have been investigated in a few studies during the last few decades.

On one side, the majority of the previous studies concentrated only on summer rainy season (JJAS). For instance, the anomalies in SSTs over the Indian and equatorial east Pacific (ENSO; El Niño–Southern Oscillation) Oceans ultimately control the interannual variability in rainfall during

summer season, where cooling/warm events produce excess/deficit of rains over the center and north of Ethiopia (Diro et al. 2011a; Gissila et al. 2004; Segele et al. 2009a, b; Korecha and Barnston 2007). In 1997, Camberlin showed that the variations in summer rainfall (June-September) over the highlands of East Africa is related to the activity of Indian monsoon.

On the other side, some of previous researches identified the link between SSTs over Gulf of Guinea and Atlantic Ocean and summer rains (Defegu 1987; Diro et al. 2011a; Segele and Lamb 2005; Wolde-Georgis et al. 2001). Moreover, the rainfall over the northern part of Ethiopia that influence the flow of the Nile River has been correlated to the overturning circulation pattern of Atlantic Ocean (Jury 2010), where the rainfall cycles showed an interdecadal variations (10-12 years).

Evidently, the teleconnections between oceanic SSTs and the main rainfall season (MAM) over the southern part of Ethiopia are much less investigated, where Diro et al. (2008) was one of the few studies to predict the rainfall (MAM) using SST anomalies over the Indian, Atlantic and Pacific Oceans. Furthermore, the secondary rainy season (SON) over the southern part of the country has not been studied.

Essentially, the Upper Blue Nile basin represents a major water source (about 60%) for the Nile River (Taye and Willems 2012). The basin had experienced both of the hydrologic extremes (droughts and floods) through the past few decades. Such floods and droughts severely affect the rain-fed agriculture that accounts for half of the country's gross production with about 85% of Ethiopian labor force (Diro et al 2011; Abegaz et al. 2007). In addition to, the lack of rainfall data in a good quality and data gaps at the records of rainfall gauges over the basin (Alhamshry et al. 2019; Fenta et al. 2018). Thus, the reliable investigations for the teleconnections between oceanic SSTs and seasonal rains at a lead time over the basin can be a matter of challenge.

Subsequently, the overall objective of this study is to enhance current knowledge about the impact of oceanic SSTs on rainfall over Ethiopia in general and the Blue Nile basin in particular. Definitely, increasing understanding for such teleconnections would be useful for improving the potential of prediction models for seasonal rainfall over the country. Consequently, such precise information or prediction models would be beneficial for an efficient management of Ethiopian water resources, especially if such a hydrologic extreme (drought) is expected, it would be valuable for other purposes such as reservoir operations, hydrological analyses, and risk assessments of soil erosion (Haregeweyn et al. 2017; Fenta et al. 2019). Otherwise, the fully understanding of rainfall variations over the Blue Nile basin would potentially assist Sudan and Egypt as downstream countries that heavily depend on the water of the Nile River.

Accordingly, specific objectives were carried out to achieve the main aim of this study as follows;

- Using various sources for rainfall data covering the country to fill the data gap appeared at rainfall records as explained in (chapter 2).
- Statistical analysis of rainfall data over both of large-scale (Ethiopia) and local-scale with considerable rainfall variations (Lake Tana), the latter is the major water source for the Blue Nile basin. This investigation on the local-scale would support the optimal use of water resources.
- Analyzing the correlation between spatio-temporal rainfall trends and global SST over certain oceanic regions, despite most of previous studies lack to relate rainfall variability to such a key predictor or large-scale driver, such as Sea Surface Temperatures (SSTs).
- Identifying the influence SST of different oceanic regions on rainfall in different seasons, such as summer (JJAS) and spring (FMAM). While, the majority of previous

studies focused only on the summer rainy season extending from June to September (JJAS) over Ethiopia.

- Dividing Ethiopia into homogeneous rainfall zones (clusters) due to the high spatial rainfall variability. New clusters were introduced in this study to improve the skill of teleconnections between SSTs and rainfall.
- Using Artificial Neural Network (ANN) as a prediction model for long-term rainfall data over Lake Tana.

1.4. Thesis outline

This thesis comprises five chapters. Chapter 1 presents the general introduction, which includes background information, description of the study area, and the problem statement and research objectives. In Chapter 2, the data source and Methodology were introduced. Chapter 3 deals with the influence of SST on rainfall over a local-scale (Lake Tana basin) and Prediction model of rainfall using ANN technique. Chapter 4 examines rainfall variability on a large-scale (whole Ethiopia) in different rainy seasons. Finally, Chapter 5 presents the overall summary and significant findings of each study, the general conclusions, and recommendations of the dissertation.

Chapter 2

Prediction of summer rainfall over the source region of the Blue Nile by using teleconnections based on sea surface temperatures

This chapter is composed based on the following paper:

Alhamshry A, Fenta AA, Yasuda H, Shimizu K, Kawai T (2019) Prediction of summer rainfall over the source region of the Blue Nile by using teleconnections based on sea surface temperatures. Theor. Appl. Climatol 137(3-4), pp: 3077-3087.

2.1. Introduction

The Blue Nile River basin, which drains the central and northwestern Ethiopian highlands, is a crucial resource for water, hydroelectric power generation, and food security for Ethiopia, Sudan, and Egypt. Even though its basin forms about 8% of the Nile basin area, the Blue Nile contributes about 60% of the Nile River flow at Aswan High Dam, Egypt (Taye and Willems 2012). The Nile River represents the only significant water resource for Egypt and Sudan (Berhane et al. 2014), and in Ethiopia the Blue Nile River supports the agricultural livelihood of millions of people (e.g., Haregeweyn et al. 2017; Sultan 2018a, b). In an effort to substantially reduce poverty and increase agricultural production, the Ethiopian government is pursuing plans for sustainable use of this water resource for irrigation and hydropower development.

Rainfall in the Ethiopian highlands is the main source of freshwater to the Nile River basin. According to Korecha and Barnston (2007), the Ethiopian highlands experience three seasonal rainfall cycles: Kiremt (June–September), Bega (October–January), and Belg (February–May). The first of these is the most important meteorological variable, accounting for 65–95% of annual rainfall totals (Gleixner et al. 2017b). Six regional climatological features control summer rainfall: (i) the meridional migration of the Inter-Tropical Convergence Zone; (ii) formation of warm lows over the Sahara and Arabian landmasses; (iii) establishment of subtropical high pressure over the Azores; (iv) cross-equatorial moisture flow from the southern Indian Ocean, central tropical Africa, and the equatorial Atlantic; (v) the upper-level Tropical Easterly Jet flowing over Ethiopia; and (vi) the low-level Somali jet (Korecha and Barnston 2007).

Given that a large part of the population relies on rain-fed farming (Diro et al. 2011a), agriculture in the Ethiopian highlands is strongly dependent on the performance of summer rainfall.

Thus, reliable and accurate predictions of summer rainfall can greatly benefit various development sectors and environmental monitoring efforts (e.g., Barnes 2017; Ebabu et al. 2018; Fenta 2016, 2017a; Gebremedhin et al. 2017) and support a drought early-warning system to meet the people's needs for food and water (Gebrehiwot et al. 2011).

Summer rainfall in many regions of Ethiopia is highly variable from year to year (e.g., Fenta et al. 2017b; Seleshi and Demaree 1995). Previous observational studies have suggested that this interannual variability is controlled by large-scale phenomena, such as the El Niño–Southern Oscillation (ENSO hereafter) (e.g., Camberlin 1995; Gissila et al. 2004; Segele and Lamb 2005; Seleshi and Demaree 1995). A modeling study by Folland et al. (1986) also suggested that SSTs in the Pacific and Indian oceans influence Ethiopian summer rainfall. In addition, several recent studies (e.g., Diro et al. 2011a; Gleixner et al. 2017b; Korecha and Barnston 2007) have investigated the correlation between summer rainfall in Ethiopia and SSTs in various regions.

Most of the previous studies depended on SSTs as a predictor of seasonal rainfall. For instance, Gleixner et al. (2017a) showed that 50% of summer rainfall in Ethiopia is influenced by variability in the equatorial Pacific SSTs. Segele and Lamb (2005) found that SSTs in the tropical Pacific and western Indian Ocean influence the onset and the cessation of summer rainfall, respectively. Diro et al. (2011b) showed that summer rainfall in different parts of Ethiopia is related to SSTs in the equatorial Pacific, the midlatitude northwest Pacific, and the Gulf of Guinea. Other studies also reported that summer rainfall in Ethiopia is negatively correlated with East Pacific SSTs, and rainfall shows a deficit during El Niño years (e.g., Diro et al. 2011a; Gissila et al. 2004; Korecha and Barnston 2007).

Most previous studies have concentrated on rainfall prediction over all of Ethiopia or the entire Blue Nile basin (e.g., Berhane et al. 2014; Diro et al. 2011a, b; Gleixner et al. 2017a, b). However, Ethiopian rainfall teleconnections are too generalized and there is considerable variability at a more local scale (Diro et al. 2011b). Therefore, this study focused on the Lake Tana basin, representing the source region and the major tributary of the Blue Nile basin. Moreover, the Lake Tana basin serves both Ethiopia and the downstream Nile countries as a source for hydroelectric power, agriculture, livestock production, ecotourism, and other benefits (e.g., Fenta et al. 2018; Haregeweyn et al. 2017; McCartney et al. 2010). Given the rapid development of water resource projects in the basin, accurate prediction of summer rainfall over the Lake Tana basin will have significant economic implications.

Seasonal rainfall prediction methods fall into three categories: statistical, dynamical, and hybrid (Diro et al. 2011b). Previous studies have shown that the most successful seasonal prediction methods exploit the statistical correlation between rainfall amounts and SSTs in the preceding months (e.g., Diro et al. 2011a; Gissila et al. 2004; Korecha and Barnston 2007). The statistical method of prediction relies on linkages between rainfall and climate parameters, of which SST is the key predictor because it changes slowly and is strongly coupled to the atmosphere (Diro et al. 2011b). Therefore, in this study we sought to develop a predictive model for summer rainfall in the Lake Tana basin by identifying the oceanic regions for which their SSTs have strong teleconnections to summer rainfall. For this purpose, we applied a neural network model to evaluate predictions of summer rainfall from SSTs in these oceanic regions at useful lead times. This process began by evaluating teleconnections to various climatic indices, then by analyzing the components of the most promising indices.

2.2. Study area

The Lake Tana basin covers an area of about 15,000 km^2 in northwestern Ethiopia, between latitudes 10.95° and 12.78°N and longitudes 36.89° and 38.25°E (Figure 2.1a). Approximately 66 km wide and 84 km long, Lake Tana is the largest lake in Ethiopia and the third largest in the Nile basin. It has a surface elevation of 1,800 m, an area of about 3,000 km^2, and a maximum depth of 15 m (Kebede et al. 2006). The basin has a complex topography, with elevations ranging from 1,780 to 4,110 m (Figure 2.1b).

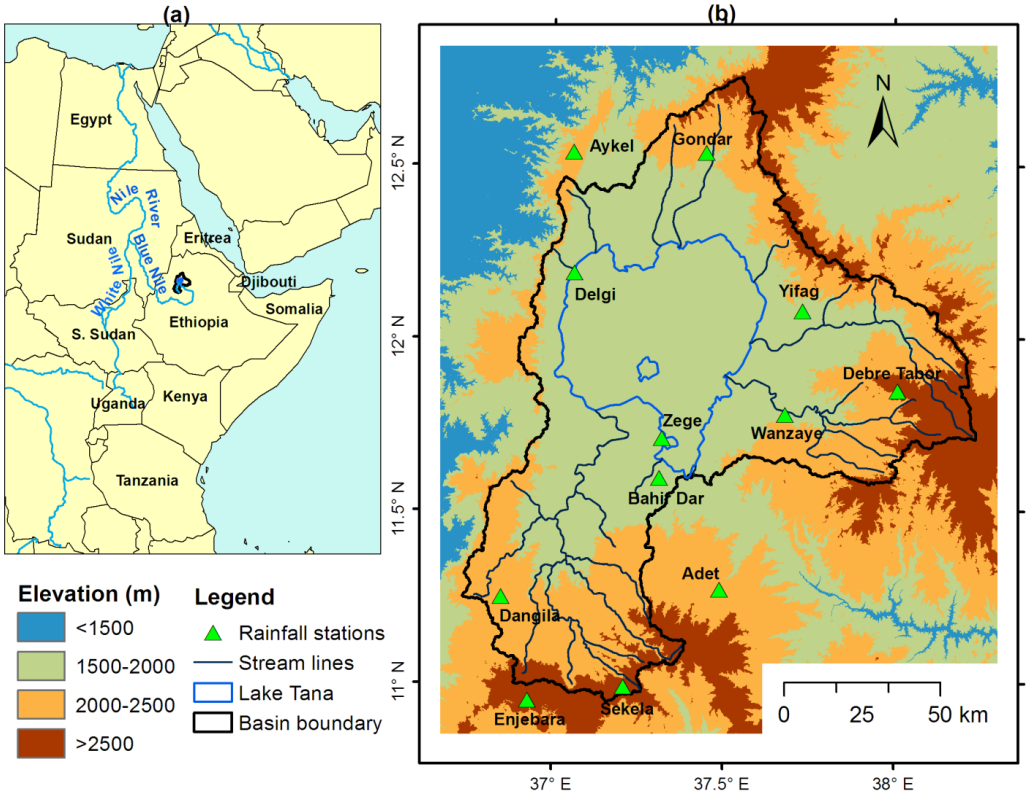

Figure 2.1 (a) Location map of northeastern Africa showing the study area in northern Ethiopia and (b) map showing the topography of the Lake Tana basin and locations of rainfall gauging stations. Elevations are extracted from the Shuttle Radar Topographic Mission (SRTM) 30-m digital elevation model.

The mean annual rainfall in the study area is 1,272 mm, of which 1,024 mm, or 80.5%, occurs in the summer rainfall season. Rainfall is mainly concentrated from June to September and is greatest in July and August, corresponding with the lowest coefficient of variation (Figure 2.2). When normalized with respect to the long-term (1985–2015) average, the annual summer rainfall tended to alternate between dry and wet years between 1985 and 1998 and to vary randomly between dry and wet in later years (Figure 2.3). Lyon (2014) documented significant variations in annual rainfall over west-central Ethiopia, conditions being relatively wet during the 1950s and 1960s and increasingly dry starting in the 1980s, accompanied by increased drought. This record emphasizes the high spatial variability of rainfall in the Lake Tana basin due to its complex topographic and geographic setting.

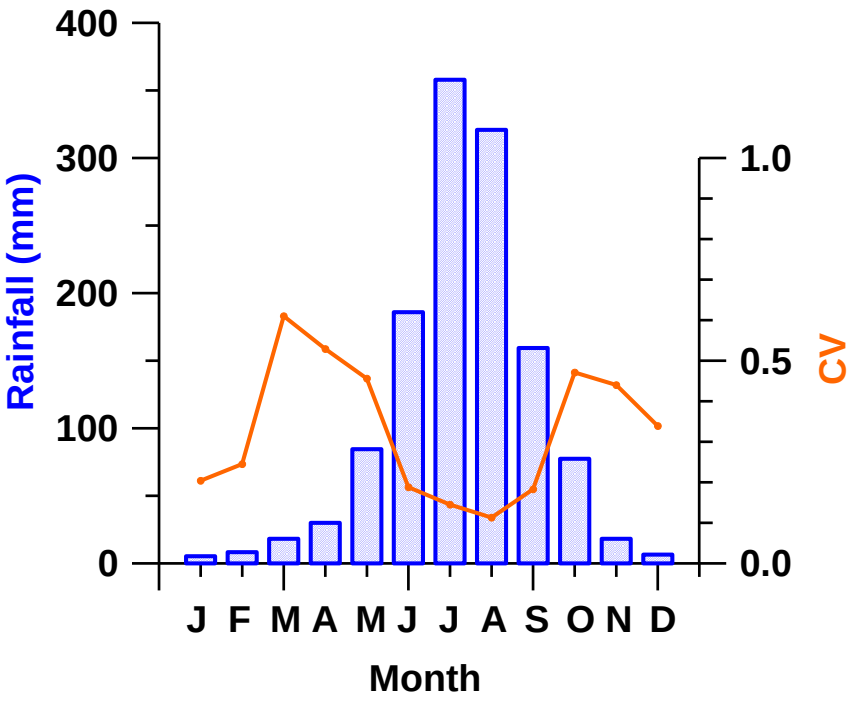

Figure 2.2 Monthly average rainfall and coefficient of variation (CV) of rainfall in the study area.

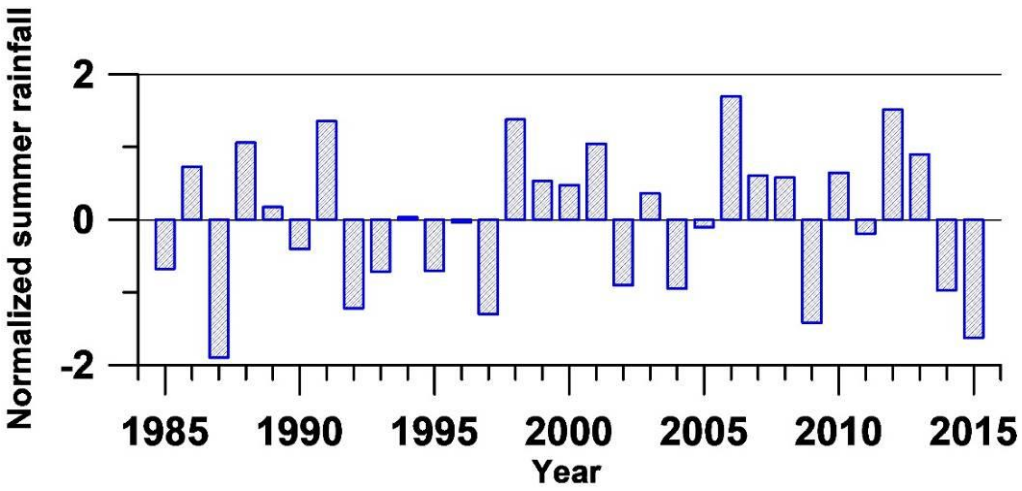

Figure 2.3 Summer rainfall in the study area normalized with respect to the 1985–2015 average.

2.3. Data and methods

2.3.1. Data sources

2.3.1.1. Rainfall data

For this study, three sets of monthly rainfall data were considered covering the period 1985–2015. The first set consists of in situ measurements from 12 rain gauges within and near the basin (locations in Figure 2.1) provided by the Ethiopian National Meteorological Agency. The second set is the satellite estimates in the Climate Hazards group Infrared Rainfall with Station (CHIRPS) dataset version 2, with a spatial resolution of 5 km, and the third set is the precipitation data in the Climate Research Unit (CRU) database of the University of East Anglia (https://www.cru.uea.ac.uk/data).

The rain gauge data are compromised by short record lengths, discontinuities in coverage, and poor data quality. Under such circumstances, satellite rainfall estimates are viable data sources for applications in climate and hydrological studies (Fenta et al. 2018).

In this study, the reliability of the raw satellite rainfall estimates was evaluated by the strength of their correlation with the rain gauge data. The CHIRPS data were the most reliable by this measure ($r > 0.95$) for all months, and the correlation was less strong with the CRU data ($r > 0.8$). Moreover, Dinku et al. (2018) evaluated the CHIRPS dataset against 1200 reference rain gauge measurements from Ethiopia, Kenya, and Tanzania and reported that CHIRPS was better than most high-resolution satellite products of rainfall data in many regions of East Africa.

The five main data sources used in the creation of CHIRPS are (i) monthly precipitation climatology from the Climate Hazards Group (University of California) Precipitation Climatology database, at 5 × 5 km grid scale, (ii) quasi-global geostationary thermal infrared satellite observations from the Climate Prediction Center and the National Climatic Data Center, (iii) the Tropical Rainfall Measuring Mission 3B42 product from NASA, (iv) atmospheric model rainfall fields from the National Oceanic and Atmospheric Administration Climate Forecast System, and (v) in situ precipitation observations obtained from a variety of sources including national and regional meteorological services (Funk et al. 2015). More details of the CHIRPS algorithm, global and regional validation results, and example applications are given in Funk et al. (2015).

2.3.1.2. Sea surface temperatures

Global SST data were obtained from Hadley Centre Global Sea Ice and Sea Surface Temperature (HadISST) version 1.1 by the British Atmospheric Data Center (Rayner et al. 2003). This product gives monthly mean temperatures with a resolution of 1° × 1° for the period 1984 – 2015 (one year more than the rainfall data), considering lag months.

Recently, Deser et al. (2010) indicated the reliability of HadISST influence in the eastern equatorial Pacific. The HadlSST data was used for this study because of its length and its use in many previous studies that concentrated on Pacific SST links with Ethiopian summer rainfall (e.g.,

Diro et al. 2011a,b; Korecha and Barnston 2007) and the influence of SST on summer rainfall in the Blue Nile basin (e.g., Berhane et al. 2014; Elsanabary and Gan 2014).

2.3.1.3. Climatic indices

The study relied on six climatic indices as below. Five of them were selected based on the previous studies that addressed the climate variability over Africa.

The Pacific Decadal Oscillation (PDO) index describes the low-frequency variations of Pacific Ocean SST in the eastern equatorial and the northern west Pacific (Mantua et al. 1997). The PDO data were downloaded from the database of the Joint Institute for the Study of the Atmosphere and Ocean (https://jisao.washington.edu/pdo/PDO.latest).

Different studies have investigated the historical relationship between the PDO and climate, especially precipitation, drought, and stream flow as hydrological quantities (e.g., Brown and Comrie 2004; Gershunov and Barnett 1998; Hu and Huang 2009; Kurtzman and Scanlon 2007; McCabe et al. 2012; Oakley and Redmond 2014; Zhang et al. 2010). These studies concentrated on the influence of PDO phase on ENSO teleconnections.

The Southern Oscillation Index (SOI) represents the normalized mean monthly difference in sea level atmospheric pressure between Tahiti and Darwin. The SOI data were downloaded from the CRU database (https://www.cru.uea.ac.uk/cru/data/soi/). Some previous studies have shown that SOI influence rainfall variability over the Blue Nile basin in Ethiopia (e.g., Conway 2000; Taye and Willems 2012).

The Indian Ocean Dipole (IOD) index is defined as the difference between SSTs in two regions of the equatorial Indian Ocean (50–70°E, 10°S to 10°N and 90–110°E, 10°S to 0°S). The IOD index data were downloaded from the Japan Agency for Marine-Earth Science and Technology (https://www.jamstec.go.jp/frsgc/research/d1/iod/).

The close link between the presence of SST mode in the Indian Ocean and the variability of rainfall over eastern Africa has been demonstrated by Camberlin (1997), Nicholson (2017), and Saji et al. (1999).

The North Atlantic Oscillation (NAO) index is traditionally defined as the normalized pressure difference between a station in the Azores and one in Iceland. The NAO index data were downloaded from the CRU database (https://crudata.uea.ac.uk/cru/data/nao/). Some previous studies investigated the association between the rainfall variability and NAO climate index, especially in Ethiopia and southeastern Africa (e.g., Jury 2010; McHugh et al. 2001).

The Arctic Oscillation (AO) index is based on the counterclockwise circulating winds around the Arctic at around 55°N latitude. The AO index data were downloaded from the CRU database (https://crudata.uea.ac.uk/cru/data/ao/). Lin et al. (2009) and Wang et al. (2005) indicated the influence of both NAO and AO on the atmospheric variability in the Northern Hemisphere.

The Mediterranean Oscillation Index (MOI) represents the normalized pressure difference between Algiers (36.4°N, 3.1°E) and Cairo (30.1°N, 31.4°E). The MOI data were downloaded from the CRU database (https://crudata.uea.ac.uk/cru/data/moi/). The influence of MOI climate index on the rainfall of Lake Tana basin in Ethiopia has been tested in our present study.

2.3.2. Methods

The Lake Tana basin was treated as a single region, consistent with many other regional-scale studies (e.g., Berhane et al. 2014; Taye and Willems 2012). Diro et al. (2011a) divided Ethiopia to five homogeneous rainfall zones and the Lake Tana basin is one part of the divided zones (northwest Ethiopia). The study was applied to 500 points on 5 × 5 km gridded CHIRPS data for the period 1985–2015.

2.3.2.1. Correlation analysis

The Pearson product-moment correlation coefficient was used to evaluate the relationship of summer rainfall with climatic indices and regional SSTs. The Student's t-test against the null hypothesis of no correlation was used to assess statistical significance (Lloyd-Hughes and Saunders 2002). Correlations $|r| > 0.36$, $|r| > 0.46$, and $|r| > 0.56$ correspond to statistical significance levels of 0.05, 0.01, and 0.001, respectively.

To investigate potential teleconnections between SSTs and summer rainfall over the Lake Tana basin, we calculated lagged correlation coefficients (r) between climatic indices and summer rainfall for lags ranging from 0 to 9 months (e.g., Kumbuyo et al. 2014; Smith et al. 2000; Yasuda et al. 2009, 2017; Yuan et al. 2016).

Cross-correlations with time lags of 4 to 5 months were considered to be most desirable for predictions of rainfall in the June–September (JJAS) period. For instance, the interannual time series of SST in January (lag of 5 months prior to the summer rainfall season) could be used as a predictor of summer rainfall (JJAS). If a strong correlation is found, it will be able to predict summer rainfall 5 months before the rainy season.

2.3.2.2. Prediction of summer rainfall from SST using Artificial Neural Network (ANN)

Our neural network model was constructed to predict summer rainfall in the Lake Tana basin on the basis of teleconnections between summer rainfall and SSTs (Elman 1990; Sfersos and Coonick 2000). Neural networks have long been used to simulate phenomena in meteorology and hydrology (e.g., Goyal and Ojha 2012; Olsson et al. 2001; Uvo et al. 1998).

Neural networks derive relationships between the inputs and outputs of a system through simple, highly interconnected processing elements (neurons) typically arranged in layers.

Furthermore, neural network can be used to connect two variables with strong degrees of nonlinearity without system dynamics. Thus, it has been applied in various fields due to its high flexibility to combine two variables (e.g., Bishop 1995; Cho 2003; Dash et al. 2010; Elsanabary and Gan 2014; Yasuda et al. 2009).

In this study, an Elman recurrent neural network was applied, a three-layer model in which the input layer represents SSTs and the output layer produces rainfall values through the hidden layer (Figure 2.4). Elman neural network has a recurrent system. The output of hidden layer is feedback to input layer and it is suitable for fitting time series, where the output of hidden layer at step (n) is transferred to the input to the network for the next step (n+1). The input and output layers, each consisting of two neurons, correspond to sequential SST and rainfall values, respectively, and the hidden layer consists of five neurons.

The connections between neurons have weight factors imposed upon them. The data (1985–2000) were used to train the network, the calculated rainfall data of the output layer being compared to the observed rainfall data, and the weight factors are then adjusted by using a back-propagation algorithm (e.g., Bishop 1995). The optimized model is then applied to the data from 2001–2015. The final optimization is defined as the best fit (strongest correlation) for the entire 1985–2015 dataset.

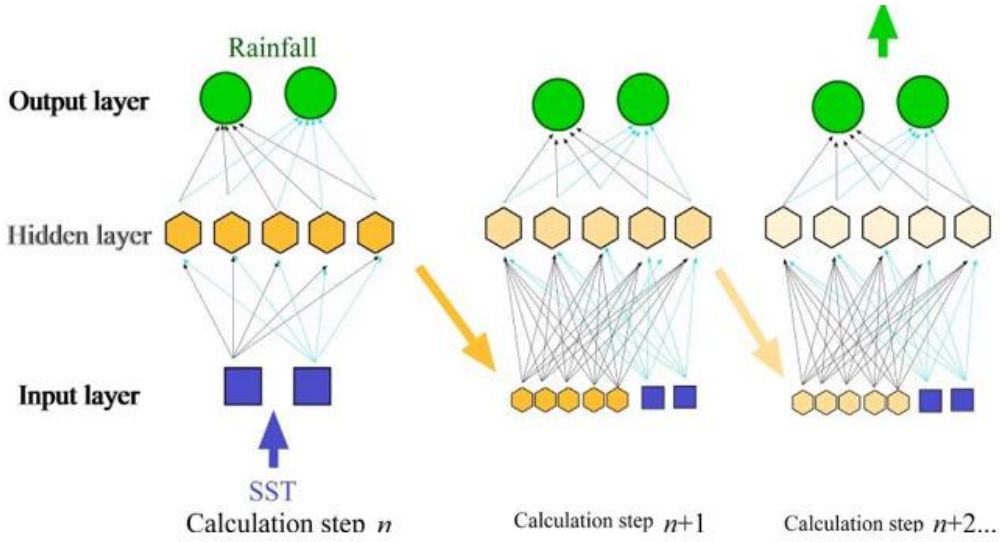

Figure 2.4 Schematic diagram showing the structure of the Elman recurrent neural network used in this study. At each iteration, the output value of the hidden layer of the previous time step is added to the input layer.

2.4. Results and discussion

2.4.1. Influence of climatic indices on summer rainfall

The correlation analysis showed that summer rainfall in the Lake Tana basin is positively correlated with SOI, MOI and AO and negatively correlated with PDO (Figure 2.5). The most consistent of these correlations is with the PDO index, with correlation values of –0.619, –0.528 and –0.407 for lags of 0, 1, and 2 months, respectively. Figure 2.6 shows the respective time series of summer rainfall and PDO at a lag of 0 month.

The results are consistent with some previous studies. For instance, Jury (2010) reported a significant correlation between PDO and summer rainfall in Ethiopia that suggested a teleconnection with Pacific Ocean SSTs. Taye and Willems (2012) reported that changes in the Pacific and Atlantic oceans influenced hydroclimatic conditions in the Blue Nile basin.

They found that annual and seasonal rainfall in the Blue Nile basin were positively correlated with SOI and negatively correlated with PDO at the 1% significance level. Conway (2000) reported that annual rainfall in the Upper Blue Nile basin had a strong positive correlation with SOI.

Korecha and Barnston (2007) showed that summer rainfall in Ethiopia was governed primarily by ENSO and secondarily by climate indicators near Africa and the Indian and Atlantic oceans.

Other studies showing a link between ENSO and Ethiopian rainfall include Abtew et al. (2009), Diro et al. (2011a, b), and Seleshi and Zanke (2004). Other studies have attempted to explain the variability of rainfall over Ethiopia using other climatic indices. For example, Camberlin (1997) linked July–September rainfall variability in the East African region to the Indian monsoon, and Jury (2010) reported that the zonal overturning circulation of the Atlantic Ocean influenced the rainfall mode over northern Ethiopia. East African climate also has been reported to be influenced by the IOD (Saji et al. 1999) and the well-known Niño 3.4 ENSO index (Indeje et al. 2000). Our results and the preponderance of previous studies emphasize the influence of the Pacific Ocean on summer rainfall in this region.

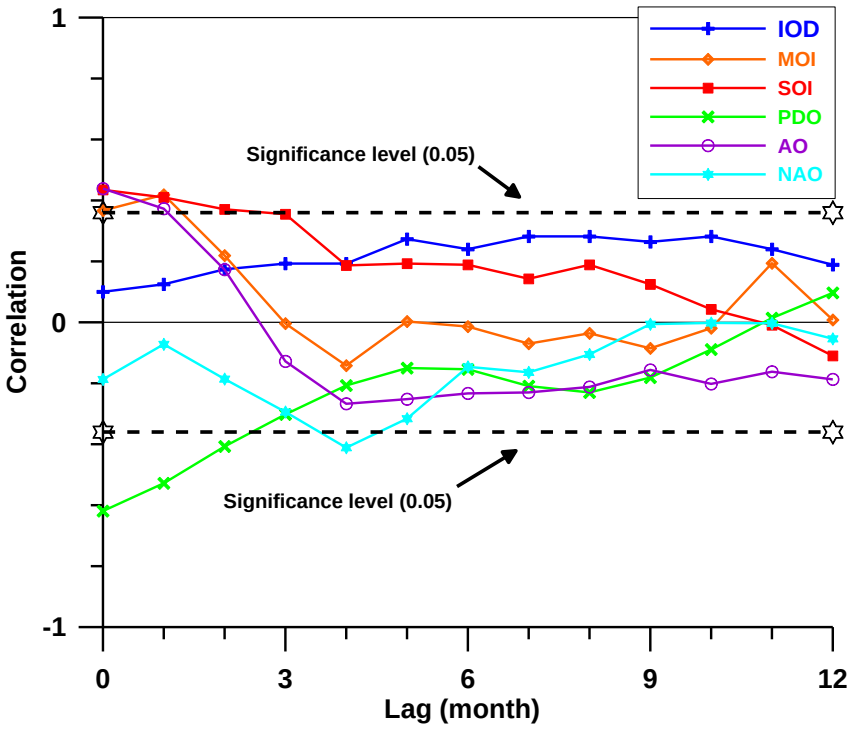

Figure 2.5 Correlations between summer rainfall in the study area and climatic indices.

The dashed lines indicate a significance level of 0.05.

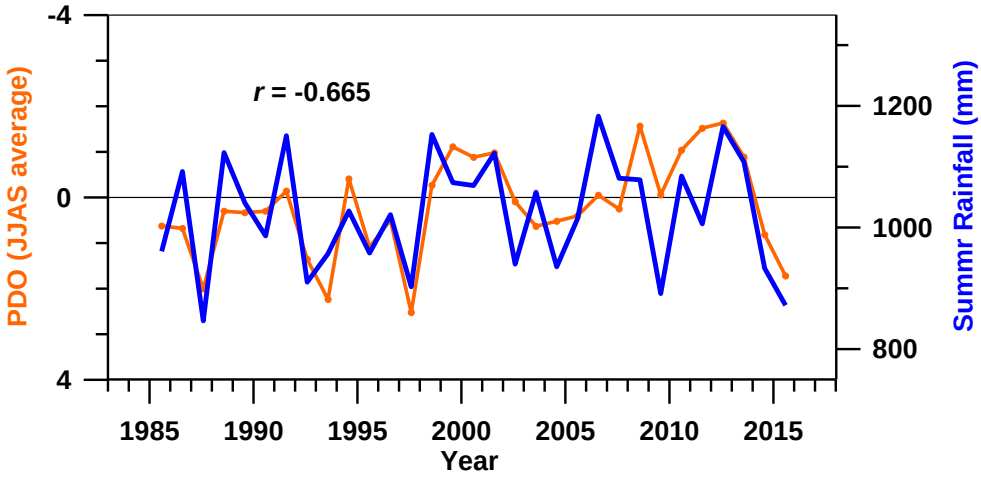

Figure 2.6 Time series of the average PDO index for JJAS (lag of 0 month) and summer rainfall in the study area.

2.4.2. Cross-correlations between summer rainfall and SST

Figure 2.7 presents the significant ($|r| \geq 0.46$) cross-correlations between summer rainfall in the Lake Tana basin and SSTs around the world during the 1985–2015 period of record for time lags of 0 to 9 months (September to the previous December). For lags of less than 5 months, large areas of negative correlation in the northeastern and western Pacific are the dominant feature in these plots. However, at longer lags the correlations are strongly positive in the western Pacific, especially for January and February, such that higher SSTs in that area coincide with more summer rainfall in the source region of the Blue Nile. In real time (no lag), significant negative correlations dominate the eastern equatorial Pacific off the coast of Peru.

Previous studies have reported that summer drought in western and central Ethiopia is associated with El Niño (e.g., Korecha and Barnston 2007; Segele et al. 2009; Seleshi and Zanke 2004), which corresponds to the rainfall signal of ENSO across the Sahel (Camberlin et al. 2010). Although variability of rainfall across the Sahel is linked to tropical Atlantic SST anomalies, the latter does not show as strong an effect on JJAS rainfall in west-central Ethiopia (Lyon 2014).

A study by Williams et al. (2012) showed that summer rainfall in parts of the Horn of Africa is associated with SST in the southern Indian Ocean. Amarasekera et al. (1997) reported that rainfall over the Blue Nile and Atbara rivers, the two main tributaries of the Nile, showed strong negative correlations with Pacific Ocean SST, accounting for the observed ENSO signature in the Nile basin. A study by Gleixner et al. (2017a) showed that 50% of JJAS rainfall in Ethiopia is influenced by variability in the equatorial Pacific SST.

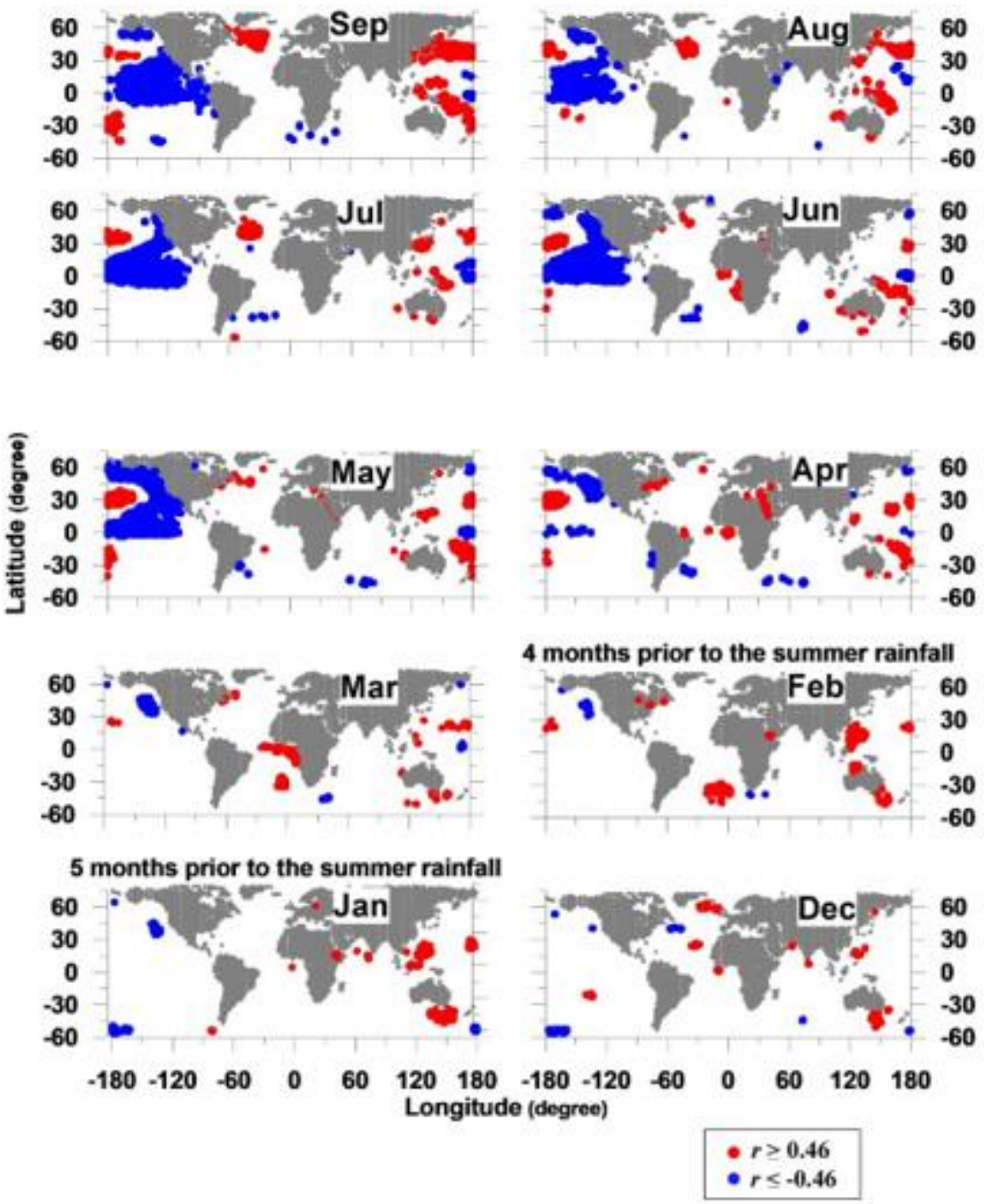

Figure 2.7 Correlations of monthly global SST with summer rainfall in the study area for 1985–2015. Correlations greater than ±0.46 correspond to significance level 0.01.

2.4.3. Prediction of summer rainfall

To investigate possibilities for summer rainfall predictions, Figure 2.8 shows two areas where SSTs in both January and February (4–5 months prior to the summer rainfall season) are significantly correlated ($|r| \geq 0.46$) with JJAS rainfall in the Lake Tana basin for the period 1985–2015, one area in the western Pacific around the Philippines and the other in the northeastern Pacific off North America.

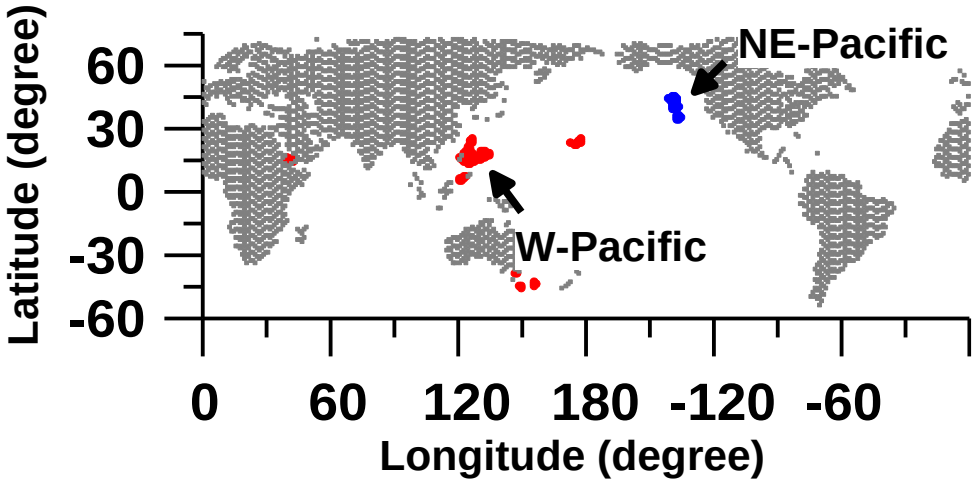

Figure 2.8 Common regions of the Pacific Ocean that are strongly correlated with summer rainfall in the study area at lags of both 4 and 5 months.

Figure 2.9 shows the time series of spatial average SST in these two regions and JJAS rainfall in the study area. A simple regression analysis showed that the correlations between these time series were strongly positive (0.629) for the western Pacific region and somewhat less strongly negative (–0.538) for the northeastern Pacific region. We take these findings as an indication of teleconnections that may make rainfall predictions possible.

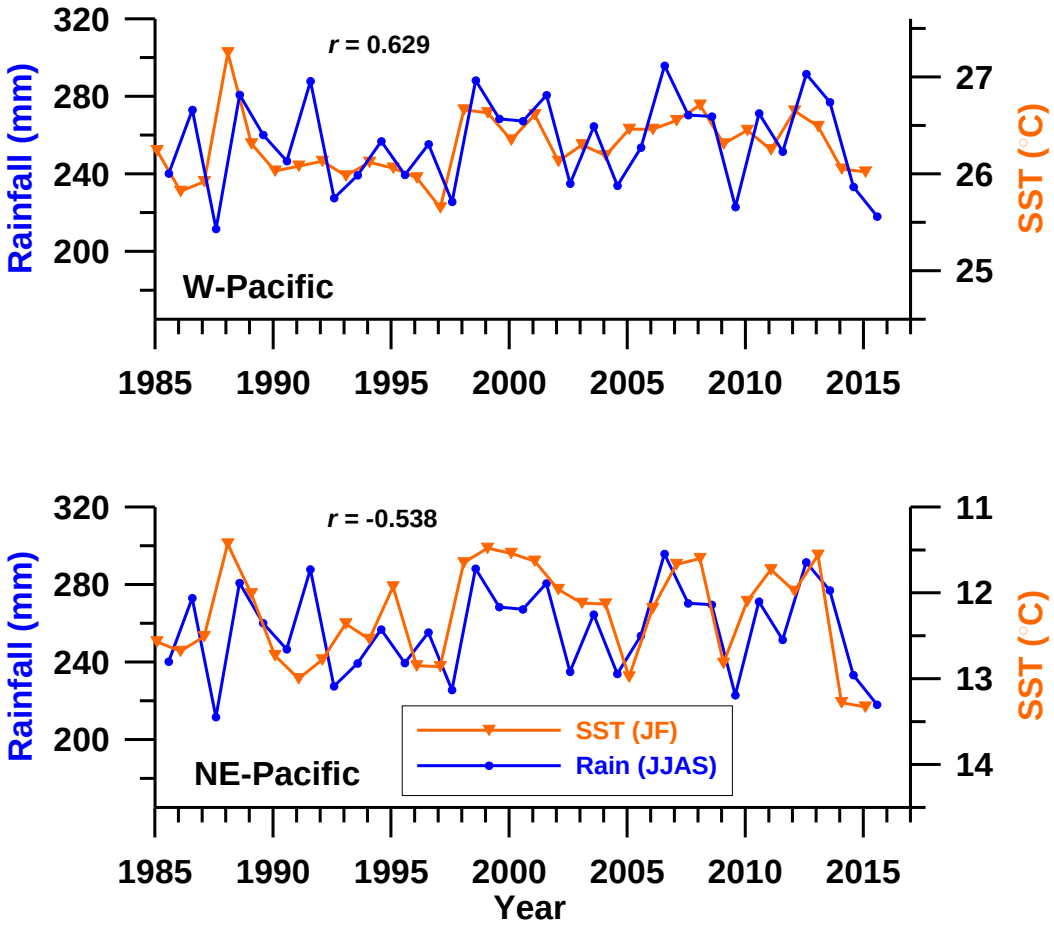

Figure 2.9 Time series showing summer rainfall in the study area and January–February SST of Pacific regions (locations in Figure 2.8).

The neural network was used to predict JJAS rainfall in the Lake Tana basin on the basis of these teleconnections (Figure 2.10). The resulting correlations, 0.817 for the western Pacific region and 0.778 for the northeastern Pacific, are about 20% stronger than the results from the simple regression analysis as shown in Figure 2.9. The improvement gained with the neural network model exceeds those offered by previous studies. For example, Elsanabary and Gan (2014) used a neural network to predict observed data for the Upper Blue Nile basin with correlations between 0.68 and 0.77.

The skill shown by the neural network is a promising development for practical purposes. Accurate predictions of summer rainfall would be very beneficial for uses such as early warnings of drought and allocation of water between Ethiopia and other downstream countries such as Egypt and Sudan. As similar models advance due to better understanding of the climatic factors, they may produce skillful predictions of summer rainfall in Ethiopia in general as well as the Lake Tana basin in particular.

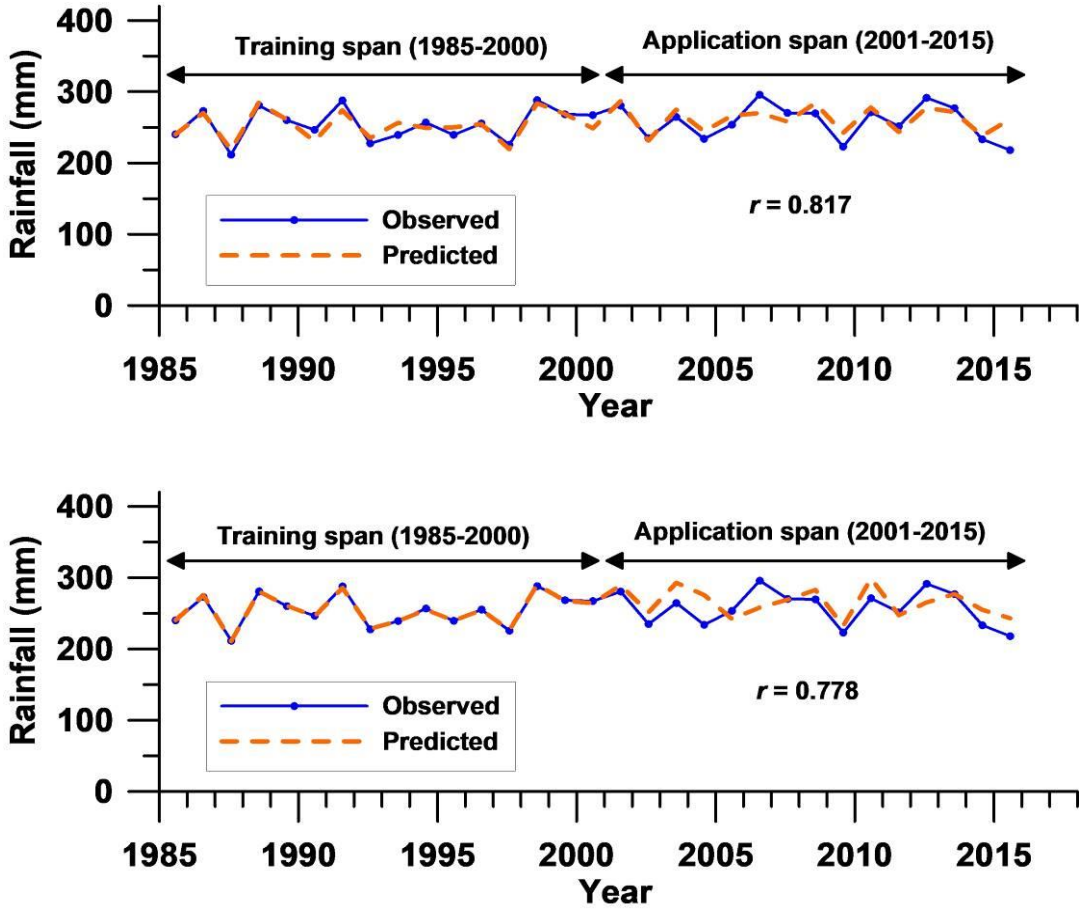

Figure 2.10 Time series of observed summer rainfall in the study area and corresponding rainfall predicted by the neural network from SST in the (a) W-Pacific and (b) NE-Pacific regions (locations in Figure 2.8).

2.5. Conclusions

Summer rainfall (June–September) accounts for about 80% of the annual rainfall in the Lake Tana basin of Ethiopia, the source region of the Blue Nile River. Prediction of summer rainfall would be valuable for managing the region's water resources and agricultural operations. This study investigated the influence of sea surface temperature (SST) as a predictor of summer rainfall in the basin by applying cross-correlation analysis between summer rainfall and climatic indices and SST in various oceanic regions from 1985 to 2015.

Summer rainfall showed a strong negative correlation (–0.619) with the Pacific Decadal Oscillation index at short time lags. Further analysis identified strong teleconnections ($|r| \geq 0.5$) between SSTs in specific parts of the Pacific Ocean and summer rainfall in the Lake Tana basin, raising the possibility of predicting summer rainfall from Pacific SSTs with a lead time of 4 to 5 months. Average SSTs of an area near the Philippines and an area west of North America were positively correlated (0.629) and negatively correlated (–0.538), respectively, with summer rainfall in the Lake Tana basin.

Predictions of summer rainfall from these teleconnected SSTs by an Elman recurrent neural network model were encouraging, indicating a strong correlation ($r > 0.77$) between the observed and predicted summer rainfall.

This study demonstrated that the developed neural network model is skillful enough to provide the basis of seasonal rainfall predictions over the basin of Lake Tana in Ethiopia, a prerequisite for early drought warnings and accurate water allocation among the nations that rely on the Nile River. To expand the scale from the basin size to country wide, the meteorological property is not homogenous. Therefore, zoning could be essential for large-scale analysis.

Chapter 3

Seasonal rainfall variability in Ethiopia and its long-term link to global sea surface temperatures

This chapter is composed based on the following paper:

Alhamshry A, Fenta AA, Yasuda H, Kimura R, Shimizu K (2020) Seasonal Rainfall Variability in Ethiopia and Its Long-Term Link to Global Sea Surface Temperatures. Water, 12(1), p.55.

3.1. Introduction

Globally, rainfall variability across time and space affects all aspects of human activity, especially agricultural economies and social activities. In particular, rainfall is the most significant meteorological parameter in Ethiopia, as approximately 85% of the Ethiopian labor force is employed in rain-fed agriculture which highly depends on low or high amounts of rainfall availability vital for crop production (Diro et al. 2011a). Moreover, the Ethiopian Electric and Power Corporation (EEPCo) declared that the local hydropower contributed to more than 98% of the energy production in 2005, 2006, and 2007 (Diro et al. 2011b).

The geographical location and topographic complexity of Ethiopia produce high rainfall variability in the region across space and time (Gamachu 1988). Spatial variations include the rainfall seasonal cycle, amount, onset, and cessation times, and length of growing season (Gamachu 1988; Segele and Lamb 2005), but sometimes, rainfall can be temporally varied from days to decades in terms of the direction and magnitude of rainfall trends over regions and seasons (Jury and Funk 2012; Seleshi and Zanke 2004).

Moreover, these spatio-temporal variations in rainfall are attributed to, in Ethiopia, the variable altitudes (Gamachu 1988) and over the Pacific, Atlantic, and Indian oceans (Segele et al. 2009a; Segele et al. 2009b; Korecha and Barnston 2007), the variable sea surface temperatures (SSTs), including the interannual and interseasonal variations in the strength of monsoon over the Arabian Peninsula (Segele and Lamb 2005; Segele et al. 2009a; Segele and Lamb 2009b).

In 2011 Diro et al. described the highlands of Ethiopia to exhibit three cycles of seasonal rainfall: spring mid-rainy season (February–May), summer rainy season (June–September), and dry season (October–January), locally known as Belg, Kiremt, and Bega seasons, respectively. In addition, Korecha and Barnston (2007) investigated the climatological factors influencing rainfall

over the region: (i) migration of the intertropical convergence zone (ITCZ) meridionally; (ii) warm lows formed over the Arabian landmasses and Sahara; (iii) formation of sub-tropical high pressure over the Azores; (iv) flow of cross-equatorial moisture from the southern, central, and equatorial parts of the Indian Ocean, tropical Africa, and Atlantic Ocean, respectively; (v) flow of the upper-level tropical easterly jet over Ethiopia; and (vi) low-level Somali jet.

Different studies have shown that SST can provide crucial predictive information regarding hydrological variability in different regions of the globe (Alhamshry et al. 2019; Yasuda et al. 2009; Tootle and Piechota 2006). For instance, most previous studies (Diro et al. 2011a; Diro et al. 2011b; Segele and Lamb 2005; Segele and Lamb 2009a; Segele and Lamb 2009b; Korecha and Barnston 2007; Alhamshry et al. 2019; Gissila et al. 2004; Camberlin 1995) have focused only on addressing the linkage between summer rains (June–September) that contribute to about 65%–95% of the total annual rainfall in Ethiopia (Gleixner et al. 2017) and global SSTs.

Generally, the majority of previous studies relied on SST as a main predictor of Ethiopian seasonal rainfall. For example, El Niño/Southern Oscillation (ENSO) as a large-scale phenomenon has a significant influence on the interannual variability of Ethiopian rains (Gissila et al. 2004; Camberlin et al. 2001; Seleshi and Demaree 1995), while the effect of SSTs of Pacific Ocean, Indian Ocean, and Gulf of Guinea on the summer rainfall of Ethiopia was indicated in (Diro et al. 2011b; Folland et al. 1986; Camberlin 1997). Meanwhile, low-level winds from the Atlantic and Indian oceans influenced rainfall of summer (Kiremt) season (Segele et al. 2009a; Segele et al.2009b; Camberlin 1995). A few of these studies indicated some correlations between SSTs over Gulf of Guinea and southern Atlantic Ocean and summer rainfall over Ethiopia (Diro et al. 2011b, Segele and Lamb 2005; Segele et al. 2009a; Segele et al. 2009b). Moreover, associations between the spring rains (March–May) as a main rainfall season over the southern part of Ethiopia and SST

are much less investigated. For example, two studies only (Diro et al. 2008; Degefu et al. 2017) used SST anomalies from the Pacific, Indian, and Atlantic oceans to predict spring rainfall.

Generally, the majority of previous studies imply that the teleconnections between SST and Ethiopian rainfall are complicated on both spatial and temporal scales and still not well investigated. Therefore, the objective of this study is directed toward more understanding the characteristics of interannual variability of rainfall in the country and investigating clearly the influence of global SSTs on Ethiopian rainfall peaks at various regions and seasons (summer and spring), to reinforce the skill of rainfall predictions that would be valuable for operations of reservoirs (Digna et al. 2018), assessment and allocation of water resources (Fenta et al. 2015; Woldesenbet et al. 2018), and for mitigation of disasters related to rainfall such as flooding and drought (Abeje et al. 2019).

Also, the better understanding of the rainfall variability plays a key role in several applications including hydrological analysis (Belay et al. 2019; Berihun et al. 2019; Fenta et al. 2017a; Fenta et al. 2017b; Sultan et al. 2018a; Sultan et al. 2018b) and soil erosion risk assessment (Ebabu et al. 2018; Ebabu et al. 2019; Fenta et al. 2016; Fenta et al. 2019; Haregeweyn et al. 2017).

For these aforementioned purposes, based on the Climate Research Unit (CRU) database of rainfall and SST data over the period 1951–2015, it would be valuable to divide Ethiopia into homogenous rainfall zones due to high spatial variability of rainfall over the country. Different previous studies have relied on principal component analysis for zonation (Ehrendorfer 1987; Dyer 1975), but this technique delivered no significant results in case of complex variability of rainfall, as in Ethiopia (Gadgil and Josh 1993).

For Ethiopia, there is no previous study for comprehensive regional zoning depending on spatial patterns of teleconnections for various seasons of rainfall. Only the summer rainfall seasons (June–September) were regionally classified in previous studies (Diro et al. 2011a; Diro et al.

2011b; Gissila et al. 2004) based on interannual correlations of rainfall amounts and homogenous annual cycles of rainfall from rain gauges.

In this regard, this study considered two main seasons (summer and spring) of rainfall over Ethiopia to define the homogenous rainfall zones based on SST to rainfall teleconnections besides other factors mentioned in a previous study (Gissila et al. 2004) such as standardized rainfall cross-correlations, annual cycles of rainfall, and geographical vicinity. Moreover, correlation analysis was applied to investigate the links between global SSTs in different oceanic regions and Ethiopian summer and spring rainfalls. SST is a main indicator because of its slowly varying rate of change and the high ocean–atmosphere coupling (Diro et al. 2011b). Finally, these significantly correlated SST areas with Ethiopian rainfall are suggested to sufficiently enhance the seasonal rainfall predictions over Ethiopia in further studies.

3.2. Materials and methods

3.2.1. Study area

The entire Ethiopian domain has an overall area of 1.13×10^6 km^2 and spans from latitude 3° to 15° N and longitude 33° to 48° E. The region is distinguished by highly complex topography in the northern and central highlands and by the lowland of the East African Rift Valley in the traversed northeast–southwest portion. Altitudes range between hundreds of meters below sea level in the northeastern regions to thousands of meters above sea level in the northern highlands (Figure 3.1).

Based on seasonal rainfall cycle, Ethiopia can be divided into three main regions: (i) northern and central western areas with one rainy season whose peak occurs in July/August; (ii) southern part with two seasons of short rainfall (September–November) and long rainfall (March–May);

and (iii) eastern and central parts of the country with two rainy periods called spring season (February–May) and summer rainy season (June–September) (Kassahun 1987).

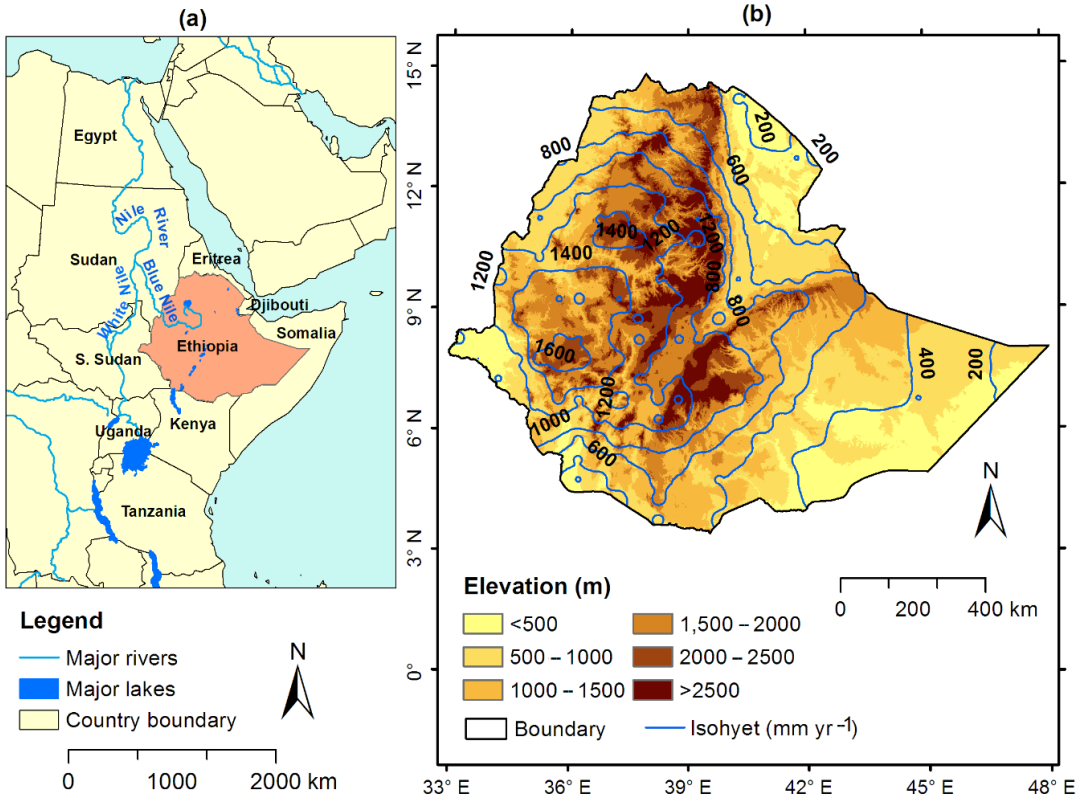

Figure 3.1 Location map of the study area: (**a**) Location of Ethiopia in eastern Africa; (**b**) A map of Ethiopia showing the mean annual rainfall distribution at 200 mm interval isohyets (blue lines) based on Climate Research Unit (CRU: https://www.cru.uea.ac.uk/data) data of 1951–2015. The background provides elevation data extracted from a 90 m resolution Shuttle Radar Topographic Mission (SRTM: http://srtm.csi.cgiar.org/).

The interannual rainfall in Ethiopia is highly variable during all seasons. Previous studies (Segele and Lamb 2005; Segele et al. 2009a; Segele et al. 2009b; Gissila et al. 2004) observed that this variability is basically influenced by large-scale phenomena (e.g., ENSO), while other studies based on modeling suggested SSTs of Indian and Pacific oceans influence Ethiopian rainfall

(Folland et al. 1986). Investigating this large-scale relation between SST of different oceanic regions and rainfall over Ethiopia is defined as teleconnection.

Definitely, rainfall is related historically to different climate parameters. However, SST is the prominent indicator due to its slow rate of change that helps for long-term investigations (Diro et al 2011b). Therefore, variable teleconnections motivate more accurate regional-scale prediction models for seasonal rainfalls over the country. The northwestern and central highlands of Ethiopia are considered main water resources not only for Ethiopia, but also for Sudan and Egypt where the Blue Nile basin contributes more than 50% of the Nile River flow (Taye and Willems 2012).

Furthermore, at highlands (>1500 m), 90% of Ethiopian people reside and depend mainly on rain-fed agriculture, with a high percentage of labor forces (89%) involved in smallholder agriculture, while the remaining population lives at lowlands (<1500 m) surrounding the highlands (Cheung et al. 2008). Crop production in Ethiopia has two cycles: (i) long-cycle crops (e.g., sorghum) are cultivated during summer and spring seasons and account for half of the national production, and (ii) short-cycle crops (e.g., barley, wheat, teff) are grown during summer and spring rainfall seasons and are responsible for 40%–54% and 5%–10% of the Ethiopian crop production, respectively (Verdin et al. 2005).

Given such a high dependence on rain-fed agriculture in Ethiopia, it becomes a vital matter to accurately identify rainfall trends and the influence of SSTs on seasonal rainfall for enhancing the seasonal prediction models within Ethiopia on a large scale, as these are expected to deliver various benefits for the development and achievement of environmental sectors planning to meet the food and water demand of its people.

3.2.2. Materials

3.2.2.1. Rainfall data

In many Ethiopian regions, existing rain gauges do not provide timely or sufficient rainfall pattern data due to the scattering of observations, uneven allocation, and data gaps in the original dataset (Fenta et al. 2017c; Fenta et al. 2018). These common problems cause inhomogeneity in the climate data series, causing an abrupt change in the average values and in series trend (Alexandersson and Moberg 1997). Additionally, gridded rainfall data have been widely used for different hydro-climatological analyses and climate variability studies (Alhamshry et al. 2019; Baigorria et al. 2007; Ghosh et al. 2009; Jury 2010; Mair and Fares 2010; Rajeevan et al. 2006).

This study relied particularly on the monthly rainfall data of about 381 rainfall grid points obtained from the CRU database (https://www.cru.uea.ac.uk/data). The data range covered 65 years of summer rainfall (1951–2015) and 50 years of spring rains (1951–2000) over Ethiopia. There are some previous studies (Tsidu 2012; Zaroug et al. 2014a; Zaroug et al. 2014b) that also showed the availability of using CRU data.

3.2.2.2. SST data

Global SST data (with resolution of 1° × 1°) used in this study covered the period (1950–2015), i.e., 1 year prior to rainfall data considering lag time. These data were provided by the Hadley Centre Global Sea Ice and SST (HadISST) version 1.1 by the British Atmospheric Data Center and described by Rayner et al. in 2003. SST represents a key indicator due to its slow rate of change, length, and intensive ocean-atmospheric coupling (Diro et al. 2011b).

Many previous studies have focused on identifying the link between SSTs at various oceanic regions and Ethiopian rainfall (Diro et al. 2011a; Diro et al. 2011b; Korecha and Barnston 2007; Alhamshry et al. 2019; Degefu et al. 2017; Deser et al. 2010).

3.2.3. Methods

3.2.3.1. Zoning of rainfall grid points

Dividing Ethiopia into homogenous rainfall zones was a crucial process due to the highly spatial variation in rainfall. Different zoning methods have been described in many studies (Gissila et al. 2004; Ehrendorfer 1987; Dyer 1975; Gadgil and Josh 1993; Diro et al. 2009). For this study though, a new division scheme was introduced based on the abovementioned rainfall data, as the standard classification of Ethiopia into three zones seemed inaccurate. The methodology followed herein was that of Gissila et al. (Gissila et al. 2004).

Briefly, in the first procedure, cross-correlation was applied to identify the relation between monthly averaged rainfalls for various grids on each zone. In the second step, the mean correlation coefficient for rainfall zones was derived. Thus, grids showing similarity in annual rainfall cycles could be categorized. Subsequently, the boundaries of each zone were adjusted through the mean inter-grid correlations between and within zones to ensure zonal homogeneity.

3.2.3.2. Standardization

Standardization was conducted for each zone to detect statistically considerable changes in rainfall, where the dependent variable of annual zone rainfall was regressed on the independent variable of time. Here, the data used covered 65 (1951–2015) and 50 (1951–2000) years for summer and spring seasons, respectively. Next, the temporal tendency was examined for statistical

significance of the Pearson correlation coefficient (*r*) following Student's *t*-test as explained in detail by Hirsch et al. (Hirsch et al. 1993). The statistical significance of the trend was evaluated (at 0.01 significance level) against the null hypothesis of no trend for the series of data.

3.2.3.3. Correlation analysis

The cross-correlation between SST at each grid point and averaged rainfall over every homogenous zone was used to identify the potential coverabilities or teleconnections between global SSTs and averaged rainfall peaks of summer July/August (JA) and spring April/May (AM) over Ethiopia. Here, the Pearson product-moment correlation coefficient (*r*) was a crucial element for evaluating the teleconnection (remote linkage) between rainfall and SST at different significance levels. The value of (*r*) varied from +1 (perfectly positive correlation) to −1 (perfectly negative correlation), while zero indicated no link. Student's *t*-test was applied against the null hypothesis of no correlation for the assessment of statistical significance (LIoyd-Hughes and Saunders 2002).

Estimation of the statistical significance of a variable in time series has been explained in different previous studies (Hirsch et al. 1993; Box et al. 1970), whereas the significance of lag-1 correlation coefficient was firstly introduced by Anderson in 1942 (Anderson 1942), followed by Kendall and Stuart in 1948 (Kendall and Stuart 1948). Higher-order lags were used when the first-order correlation insufficiently depicted the serial dependence (McCuen 2003).

For this purpose, lagged (*r*) was calculated for lags from 0 to 9 months, i.e., calculating (*r*) until October/November and July/August of the previous year to summer and spring peaks, respectively, for identification of lags that show significant correlations (Yasuda et al. 2009; Smith et al. 2000).

The normal distribution of SST data followed the distribution was explained in previous studies (Yasuda et al. 2009; Kodera 2004). Table 4.1 shows the calculated correlation coefficients |*r*| corresponding to statistical significance levels. For this study, the concentration was on the significance at 1% level (two-tailed) with the calculated correlation coefficients of 0.32 and 0.36 for summer and spring rainfalls, respectively.

Significance Level (α)	**Correlation Coefficient (*r*)**	**Correlation Coefficient (*r*)**
	Summer Rainfall (*n* = 65)	**Spring Rainfall (*n* = 50)**
0.05	0.24	0.28
0.01	0.32	0.36
0.001	0.40	0.45

Table 3.1 Calculated values of Pearson's correlation coefficient (*r*) corresponding to significance levels.

3.3. Results and discussion

3.3.1. Zoning of Ethiopia based on seasonal rainfall

Figure 3.2 displays the country of Ethiopia being divided into two main subregions: (i) northern and central regions with nine zones (1–9) for summer rainfall and (ii) southern region with five zones (1–5) for spring rains. The average cross-correlations between and within zones were tested for various times for the optimal selection of a proper number of zones, as shown in Tables 4.2 and 4.3, with a reasonable homogeneity delineating a new classification for Ethiopia into nine summer and five spring zones.

In case of high spatial and temporal variability of Ethiopian rainfall, it would be crucial to delineate boundaries and define the country into homogenous zones, as the optimal zonation would be valuable for hydrologic modeling, prediction, ecological, and climate classification, or for any other analysis (Yasuda et al. 2018; Zhang et al. 2016). For this purpose, different research studies have been undertaken. For example, Korecha and Sorteberg (Korecha and Sorteberg 2013) indicated that the National Meteorological Agency of Ethiopia divides the region into eight homogenous zones depending on the main systems of atmospheric–oceanic circulation and rain production.

Moreover, Gissila et al. (2004) grouped Ethiopia into four clusters based on seasonal rainfall cycles and homogeneity of interannual rainfalls at 24 rain gauges. Despite following the same methodology of the latter study, both this study and Diro et al.'s (2009) produced different results.

Here, the country was divided into nine summer peak (JA) zones and five spring peak (AM) zones based on CRU seasonal rainfall data covering Ethiopia (381 grid points), whereas Diro et al. (2009) delineated five homogenous summer rainfall regions (June–September) and six spring zones (February–May) depending on the data from 33 rainfall stations and considering the interannual variation of seasonal rainfalls.

Additionally, a number of recent studies carried out (Degefu et al. 2017; Tsidu 2012; Wagesho et al. 2013) obtained different zoning outcomes. Therefore, the classification of Ethiopia into homogenous zones could be different from one study to another, because of the high variability in large-scale forces producing rainfall over the country.

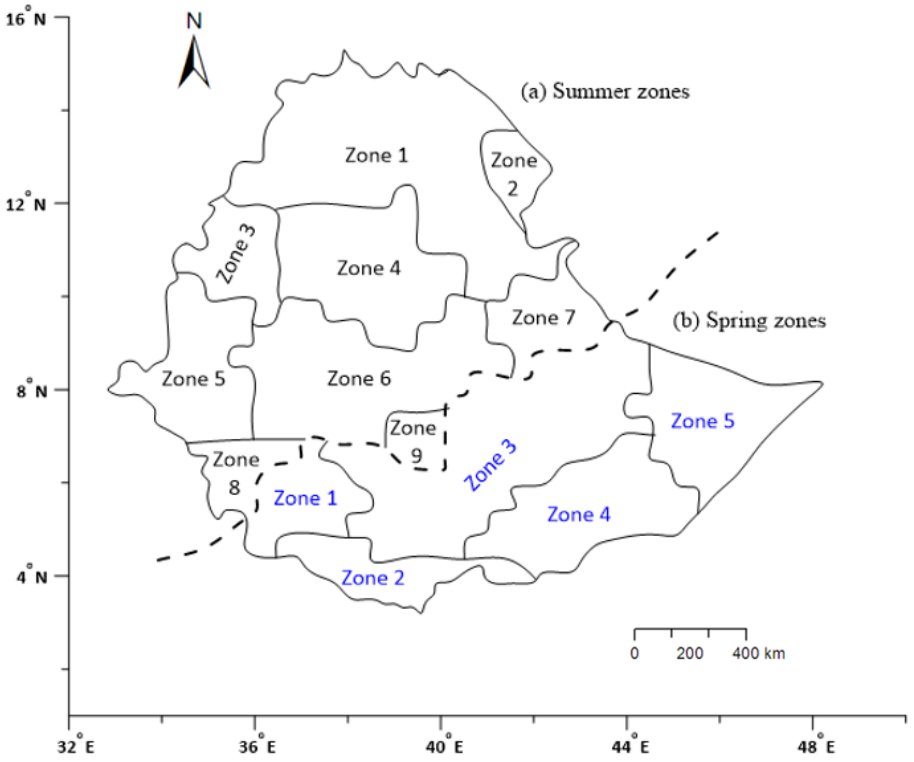

Figure 3.2 Homogenous rainfall zones over Ethiopia obtained from correlation analyses using monthly rainfall variability of summer rainfall peaks July–August (JA) and spring rainfall peaks April–May (AM).

Summer zones	1	2	3	4	5	6	7	8	9
1	1.000	--	--	--	--	--	--	--	--
2	0.361	1.000	--	--	--	--	--	--	--
3	0.603	0.548	1.000	--	--	--	--	--	--
4	0.786	0.371	0.676	1.000	--	--	--	--	--
5	0.274	0.748	0.473	0.374	1.000	--	--	--	--
6	0.409	0.536	0.863	0.436	0.371	1.000	--	--	--
7	0.164	0.240	0.586	0.107	0.140	0.683	1.000	--	--
8	0.305	0.332	0.531	0.325	0.388	0.387	0.302	1.000	--
9	0.369	0.146	0.630	0.359	0.144	0.324	0.397	0.562	1.000

Table 3.2 Mean cross-correlation (mean inter-grid correlation) between and within nine summer zones.

Spring Zones	1	2	3	4	5
1	1.000	-	-	-	-
2	0.067	1.000	-	-	-
3	0.596	0.556	1.000	-	-
4	0.690	0.174	0.649	1.000	-
5	0.211	0.702	0.604	0.550	1.000

Table 3.3 Mean cross-correlation (mean inter-grid correlation) between and within five spring zones.

3.3.2. Temporal variation of rainfall

3.3.2.1. Annual rainfall cycle

Figure 3.3 shows the mean monthly rainfall values calculated for each zone. Apparently, the northern and central Ethiopian regions displayed a regime of monomodal summer rainfall cycle (June–September) with rainfall peaks in July/August (hereafter JA), which is consistent with that reported by Diro et al. (2011b). In contrast, the southern region of the country experienced bimodal rainfall cycles for spring or long rainfall (March–May) with rainfall peaks in April/May (hereafter AM) and another short rainfall cycle from (October–November).

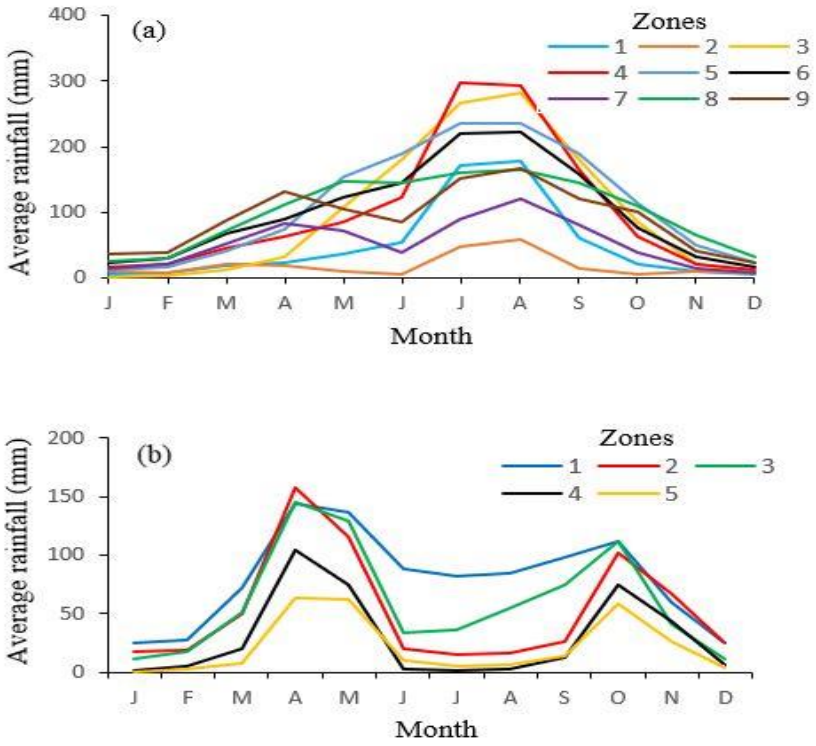

Figure 3.3 Mean monthly rainfall over Ethiopia for (**a**) nine summer zones (1951–2010) and (**b**) five spring zones (1951–2000).

3.3.2.2. Interannual rainfall variability

Figure 3.4a shows a time series of standardized summer rainfall variability for each zone from 1951 to 2015 with a considerable variation between wet and dry years from one zone to another. The northern and central rainfall zones displayed a successive time period of 2–4 years of dry and wet years without any distinct trend, in addition to three records of drought years in 1965, 1984, and 2002. Moreover, the magnitude of the series gradually decreased for all zones, except for the central zones (7 and 8).

Figure 3.4b indicates the time series of standardized spring rainfall variability for each zone from 1951 to 2000, where the eastern and southern zones indicated a continual below-average

amount of rainfall from 1952 to 1956, but recovered in the late 1950s. Moreover, the drought years appeared in 1974, 1980, and 1984 with a prevalent drier condition from the beginning of the 1990s.

Both figures also confirmed Ethiopia's significant interannual rainfall variability with the year 1984 being the major year of drought that covered the whole of Ethiopia (Seleshi and Zanke 2004), in which the standard deviations varied between 0.7-below-average in the southern zones and greater-than-2 below-average in the northern zones. Moreover, the country experienced abundant amounts of rainfall for 4 years (1951, 1961, 1967, and 1982) of the given 65 years for the study.

These results were consistent with Seleshi and Zanke (2004) for their analysis of the annual rainfall totals and annual rainy days over the country. The Ethiopian rainfall variability has been described in numerous studies, depending on the leading mechanisms of the ITCZ migration, influences of topography, and various interactions of hydro-climate system on regional scales (Seleshi and Zanke 2004; Griffiths 1972).

3.3.3. Teleconnections

3.3.3.1. Cross-correlation between summer rainfall (July/August Peak) and oceanic SSTs

Firstly, for the 65 years of summer rainfall (1951–2015), the correlation coefficients ±0.24, ±0.32, and ±0.40 corresponding to significance levels of 0.05, 0.01, and 0.001 were calculated using two-tailed *t*-test. As shown in Figure 3.5, the common summer rainfall zones having the same significantly correlated SST regions were statistically extracted and represented at significance levels. In particular, this study relied on the 0.01 significance level with $r = \pm 0.32$, showing a significantly strong correlation at a lag time of 5–8 months between the July/August rainfall and SST at the nine zones. Positive and negative correlations were represented in red and blue colors, respectively (Figure 3.5).

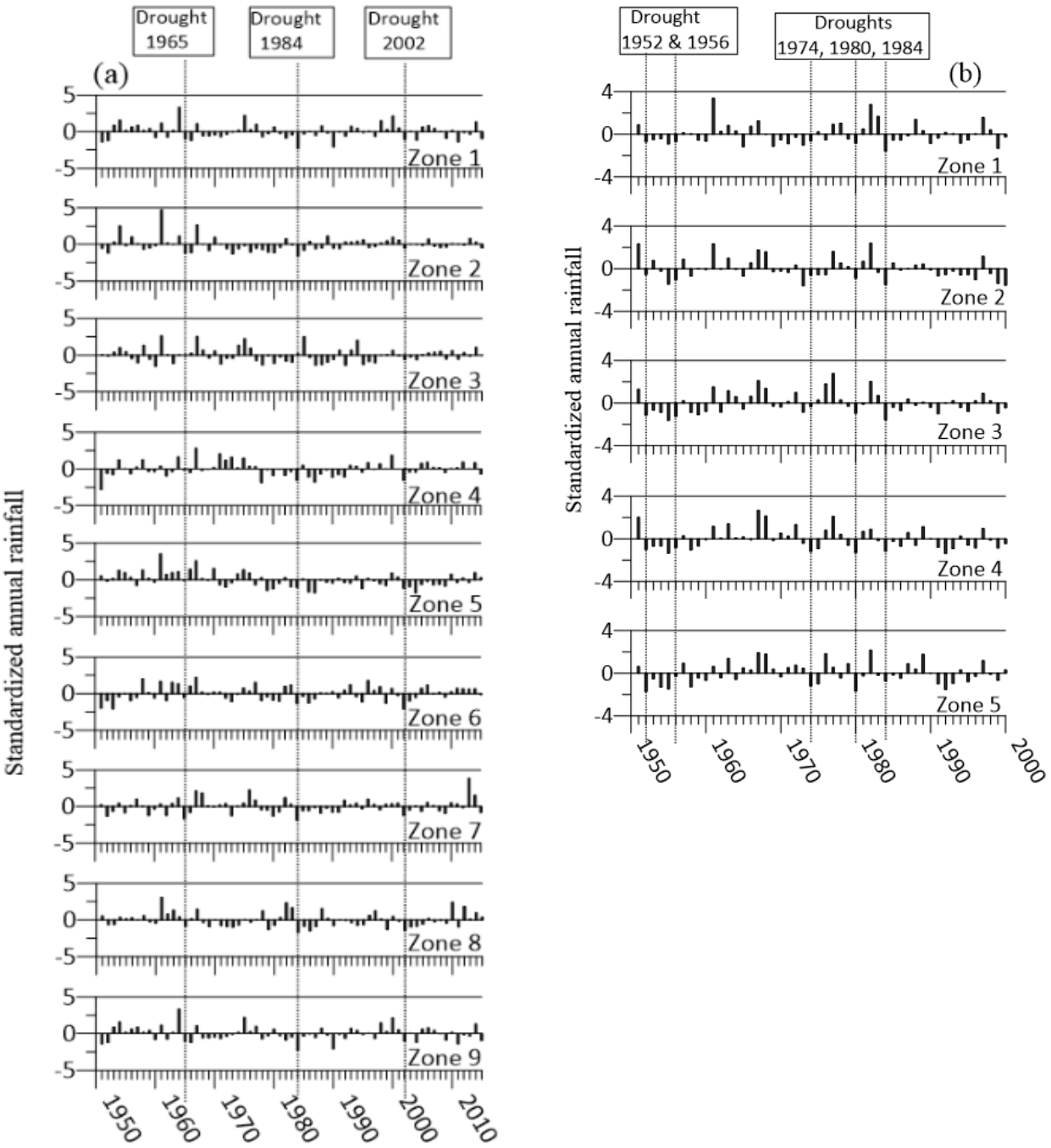

Figure 3.4 Standardized time-series plot of annual rainfall totals for (**a**) summer rainfall zones (1951–2015) and (**b**) spring rainfall zones (1951–2000).

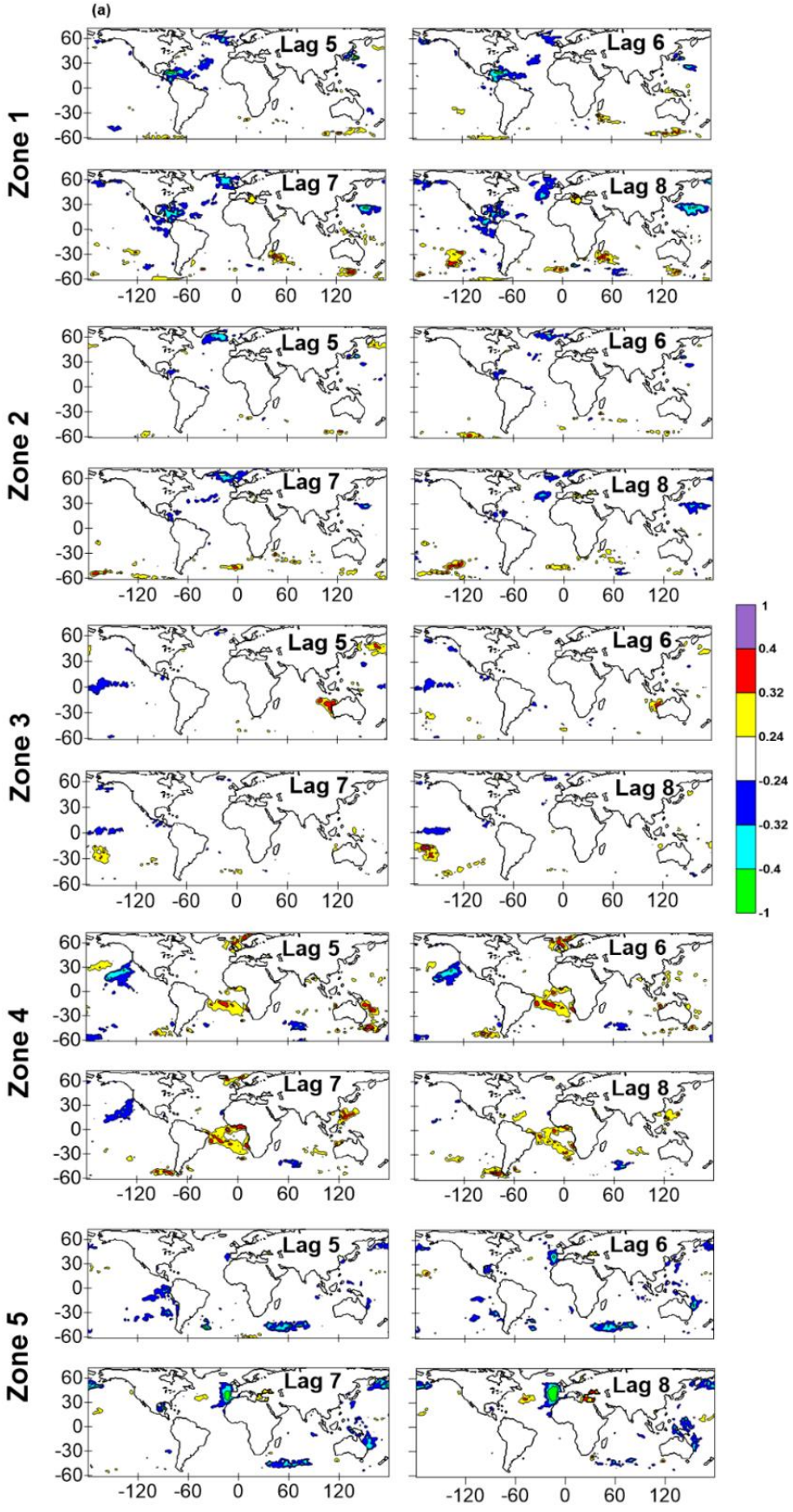
(a)
Zone 1
Zone 2
Zone 3
Zone 4
Zone 5
Lag 5
Lag 6
Lag 7
Lag 8
60
30
0
-30
-60
-120 -60 0 60 120
1
0.4
0.32
0.24
-0.24
-0.32
-0.4
-1

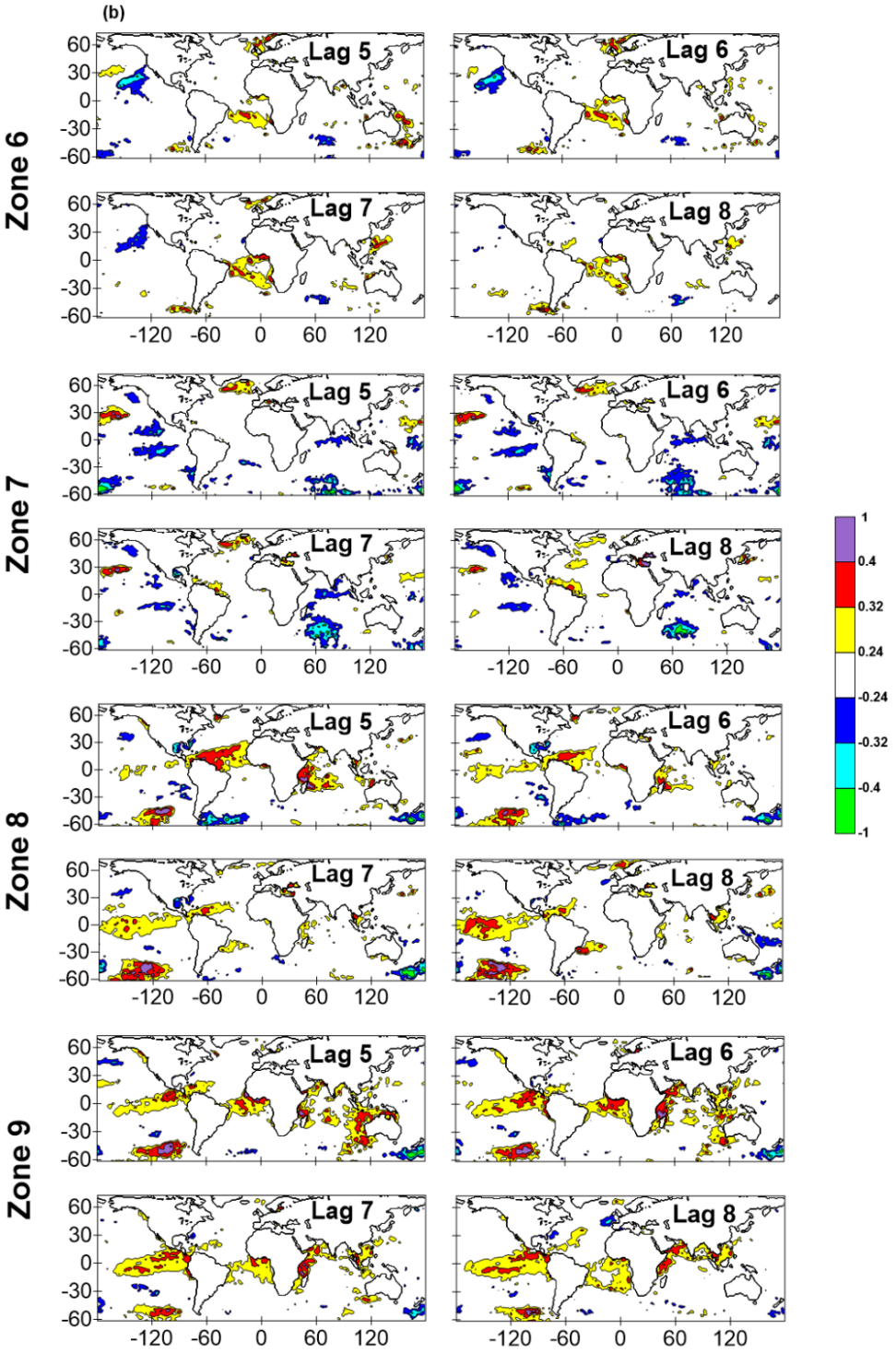

Figure 3.5 Maps (**a**) and (**b**) showing the nine summer rainfall zones with cross-correlations between July/August summer rainfall of each zone and sea surface temperatures (SSTs) for different oceanic regions at lag times of 5–8 months.

From the standpoint of forecasting, possible correlations of SST with rainfall at longer lag times are potentially effective. For instance, as shown in the left side of (Figure 3.6), at 5–6 months lag period, Gulf of Guinea SST showed a significantly positive correlation with July/August rainfall in the central zones (6 and 9), while two regions in the Pacific Ocean exhibited the strongest teleconnection (positive and negative) between SST and rainfall at zones 8 and 9, due to the well-known Pacific events of ENSO.

A recent investigation of Gleixner et al. (2017) revealed that half of Ethiopian summer rainfall is affected by the variation of equatorial Pacific SST. Additionally, various previous studies indicated the teleconnection between SST of the Pacific and Ethiopian summer rainfall (Diro et al. 2011a; Segele and Lamb 2005; Korecha and Barnston 2007; Gissila et al. 2004; Camberlin 1997; Block and Rajagoplan 2007) and excess of rainfall during spring season.

At 6–7 months lag period, the central summer rainfall zones 4 and 6 indicated a significantly positive correlation with both Gulf of Guinea and a small area over the southeastern part in the Pacific. Diro et al. (2011b) identified the effect of the Pacific SST on rainfall, besides the influence of the Gulf of Guinea, over different parts of Ethiopia.

The strongest influence of southern Indian Ocean SST on Ethiopian rainfall due to Ethiopia's location was indicated at rainfall zones 5 and 7 (right side of Figure 3.6); however, the effect of the Indian Ocean SST was disregarded, as the study's objective was directed toward the remote influence (teleconnection) of oceanic SST on Ethiopian rainfall.

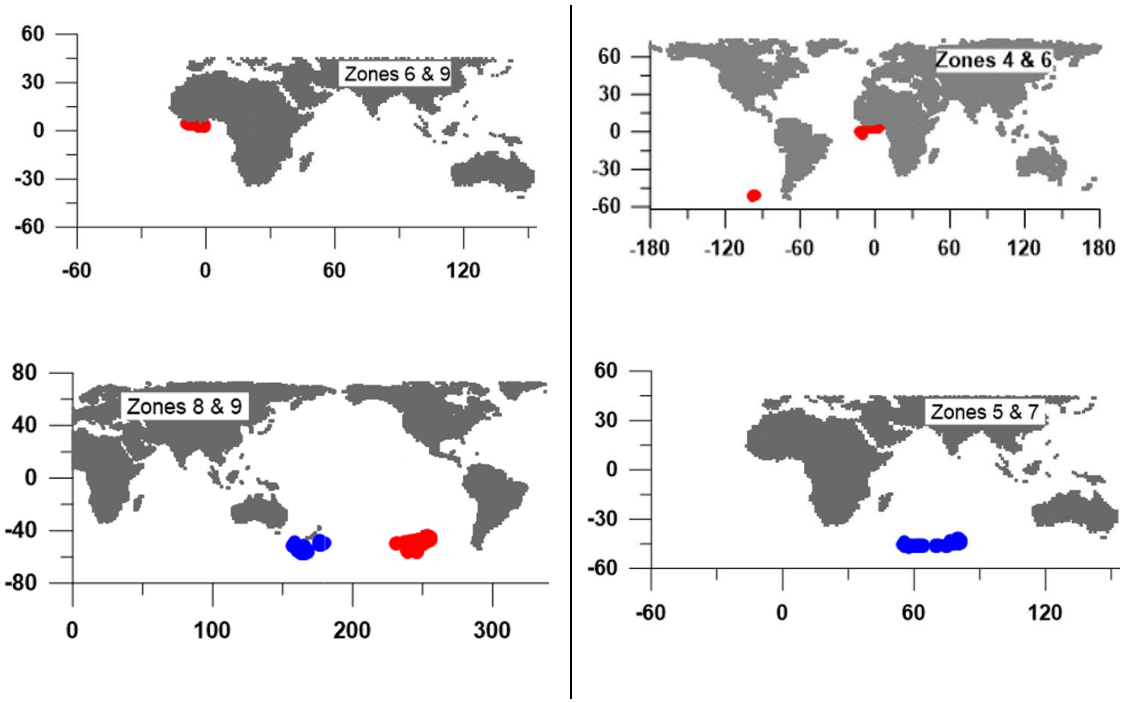

Figure 3.6 Extraction of common summer rainfall zones having the same significantly correlated SST regions ($r \geq 0.32$) at lag times of 5–6 months (left side) and 6–7 months (right side). Red and blue colors indicate positive and negative correlations, respectively.

For the northern summer zones 1 and 2, the northwest Pacific showed insignificant influence on rainfall (negative correlation) at a lag time of 7–8 months (Figure 3.7). In 2005, Segele and Lamb indicated that upper-level features such as the African easterly jet (AEJ), and tropical easterly jet (TEJ) affect summer rainfall over Ethiopia based on their strength and location. Moreover, moisture flux from the Atlantic and Indian oceans and as a lower-level circulation affected by the highs of Mascarene and St. Helena affects summer rainfall significantly (Kassahun 1987).

Generally, various previous studies (Diro et al. 2011a; Diro et al. 2011b; Camberlin 1995; Asnani 2005; Bekele 1997) identified the teleconnection between SST of the Indian Ocean and Ethiopian rainfall, also they suggested that sea surface temperature anomalies (SSTA) of eastern

part of Pacific Ocean may affect summer rainfall as a main rainy season. These positive SSTAs are associated with deficits in summer rainfall and excess of rainfall during spring season.

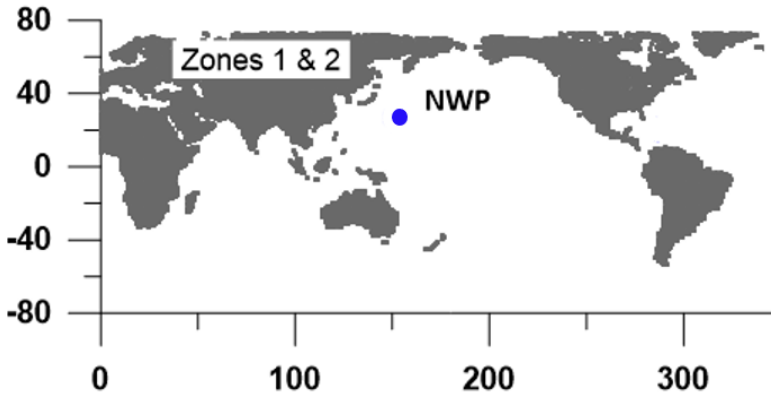

Figure 3.7 Extraction of common summer rainfall zones having the same significantly correlated SST regions ($r \geq 0.32$) at the lag time of 7–8 months.

3.3.3.2. Cross-correlation between spring rainfall (April/May Peak) and oceanic SSTs

As shown in Figure 3.8, the common spring rainfall zones having the same significantly correlated SST regions were statistically extracted and represented at significance levels. In particular, this study relied on the 0.01 significance level with $r = \pm 0.36$, showing a significantly strong correlation at the lag period of 5–8 months between April/May rainfall and SST at five zones.

From the standpoint of prediction, possible correlations of SST with rainfall at longer lag times are potentially effective. For instance, at lag time of 6–7 months, the northern Atlantic Ocean SST showed a significantly negative correlation with spring rainfall zones 3 and 5 representing southern and southeastern regions of Ethiopia (left side of Figure 3.9).

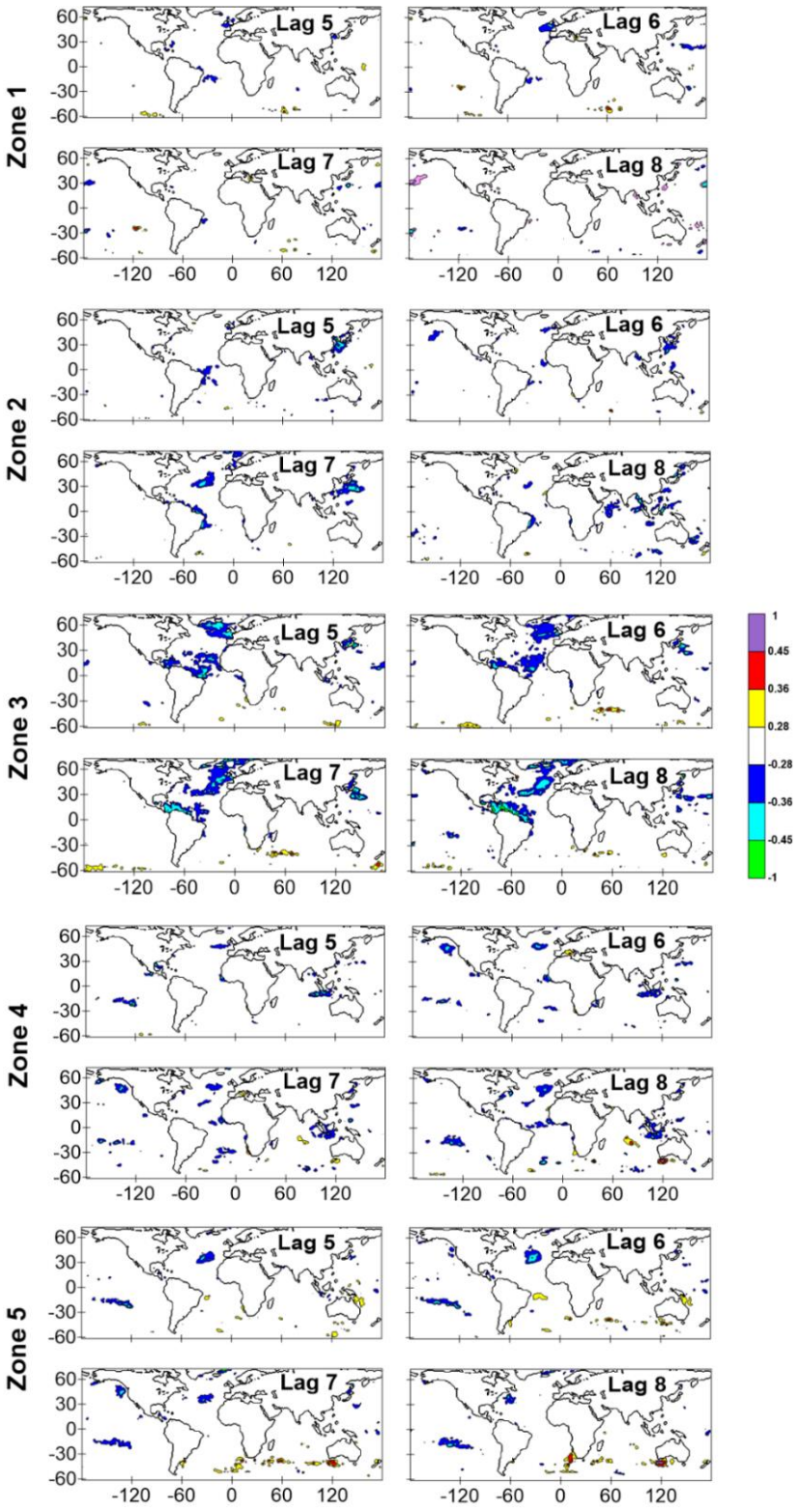

Figure 3.8 Maps showing the cross-correlations between April/May spring rainfall of each zone and SSTs for different oceanic regions at a lag time of 5–8 months.

Moreover, at 7–8 months, two regions at the southern Indian Ocean exhibited a strong positive influence on spring rainfall due to Ethiopia's location for the southeastern zones 4 and 5 (right side of Figure 3.9).

The passage of ITCZ controls the shape of seasonal rainfall cycle. Annually, it oscillates from 15° N in July to 15° S in January and back again causing monomodal and bimodal rainfall patterns over northern and southern parts of Ethiopia, respectively (Asnani 2005). In addition to the difference between the land surface and Indian Ocean in the heat capacity inducing ITCZ's meridional arm. The latter produces rainfall during February and March over the southwestern part of Ethiopia (Kassahun 1987). Additionally, the strength and location of upper-level feature of the subtropical westerly jet (STWJ) affects spring rainfall over the country (Segele and Lamb 2005).

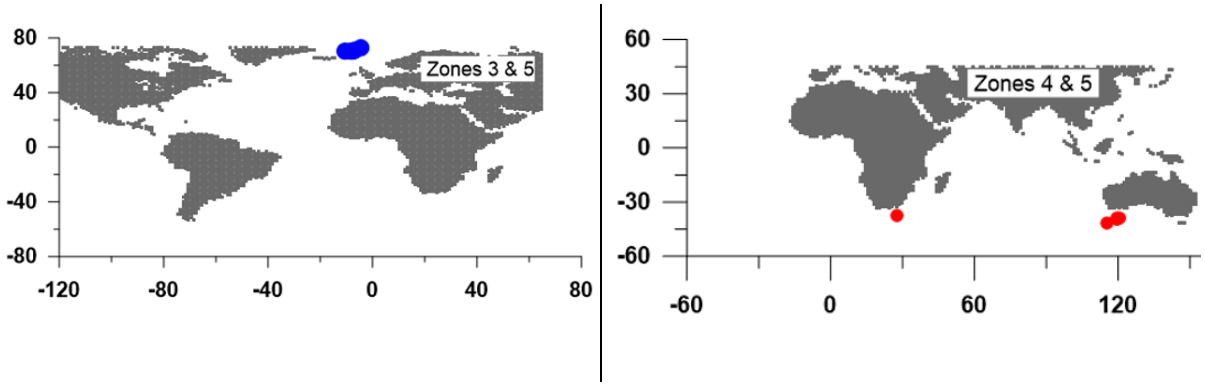

Figure 3.9 Extraction of common spring rainfall zones having the same significantly correlated SST regions ($r \geq 0.36$) at a lag time of 6–7 months (left side) and 7–8 months (right side). Red and blue colors indicate positive and negative correlations, respectively.

Generally, SST and spring rainfall teleconnections are spatially and temporally complicated, where Diro et al. 's (2008) was the only previous study to investigate the influence of SSTs of the Pacific, Atlantic, and Indian oceans on spring rains (March–May), depicting the main rainfall season over the southern part of Ethiopia. Therefore, the results in this study provide a more

detailed understanding of such teleconnections that would be valuable for enhancing rainfall prediction system over Ethiopia.

Finally, to visualize the SST regions showing significant correlation with seasonal rainfall over Ethiopia, the correlation coefficients between rainfall time series and SSTs were derived for the aforementioned summer and spring zones with significant correlations (Figures 3.10 and 4.11). These regions could be used as inputs for a forecasting model for further studies at a lead time before the rainfall season.

For the summer season, a significant correlation was indicated ($r \geq \pm 0.37$) at a lag time of 5–6 and 6–7 months prior to the rainy season. In particular, summer zones (8 and 9) at 5–6 months lag period indicated opposite sense of positive and negative correlations, with the difference in SSTs enhancing the correlation. Thus, both zones (8 and 9) exhibited the strongest correlation ($r \geq 0.46$) between summer rainfall and SST among all other summer zones (Figure 3.10).

On the other side, the spring rainfall zones (3 and 5) also showed significant correlation ($r \geq -0.40$) at 6–7 months lag time, representing the influence of northern Atlantic Ocean SST, while the southern Indian Ocean SST exhibited the strongest correlation ($r \geq 0.5$) at 7–8 months of lag time (Figure 3.11).

These results suggest that SSTs of the southern Pacific and northern Atlantic oceans could be effective as inputs for prediction models of Ethiopian summer and spring rainfalls, respectively, at a lead time before these seasons.

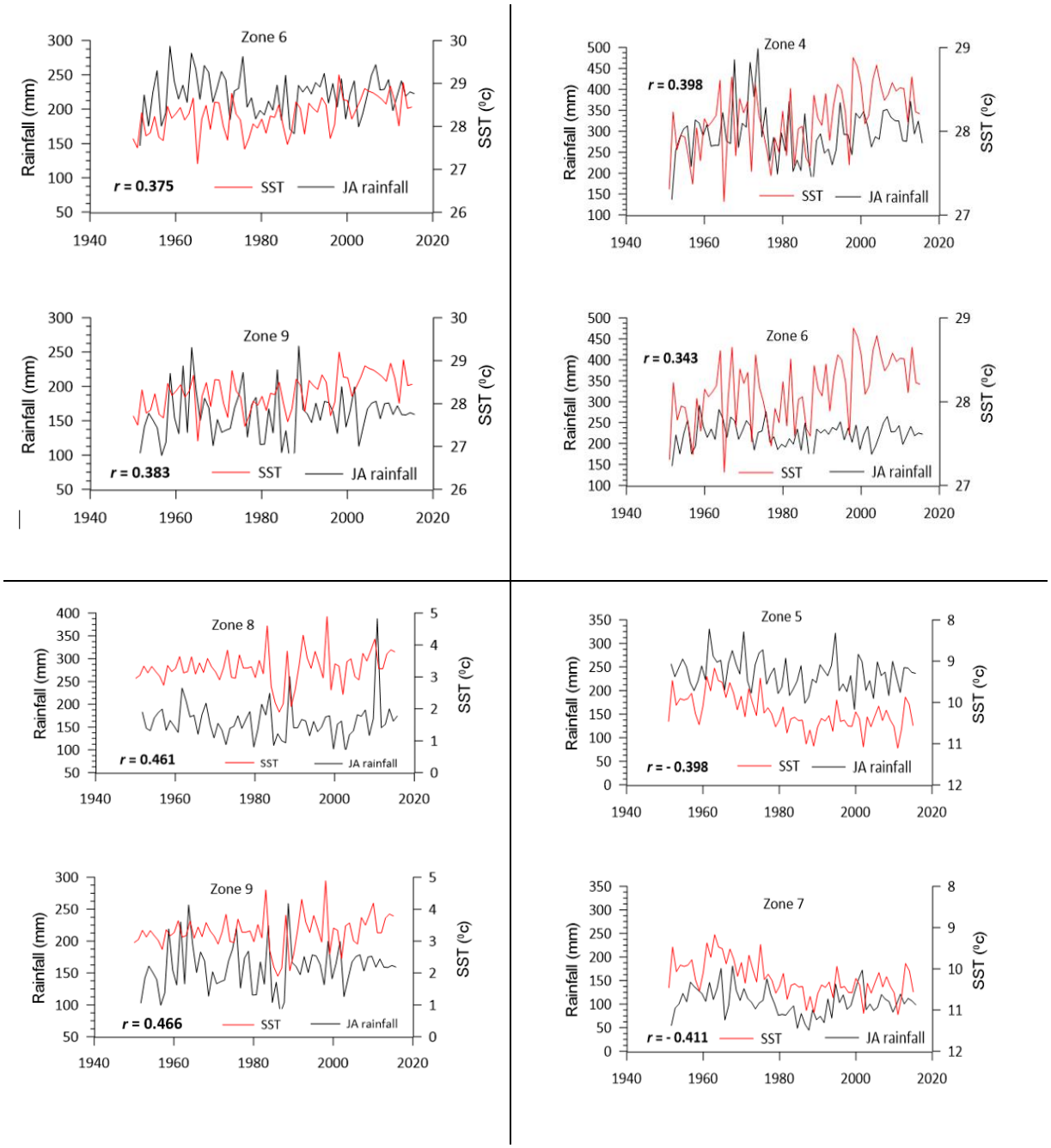

Figure 3.10 Significant cross-correlations between selected summer rainfall zones and oceanic SSTs at lag times of 5–6 months for zones (6 & 9) and (8 & 9) (left side) and 6–7 months for zones (4 & 6) and (5 & 7) (right side) for the rainfall time series (1951–2015). Zones 8 and 9 show the calculated (*r*) by subtracting positive and negative correlations.

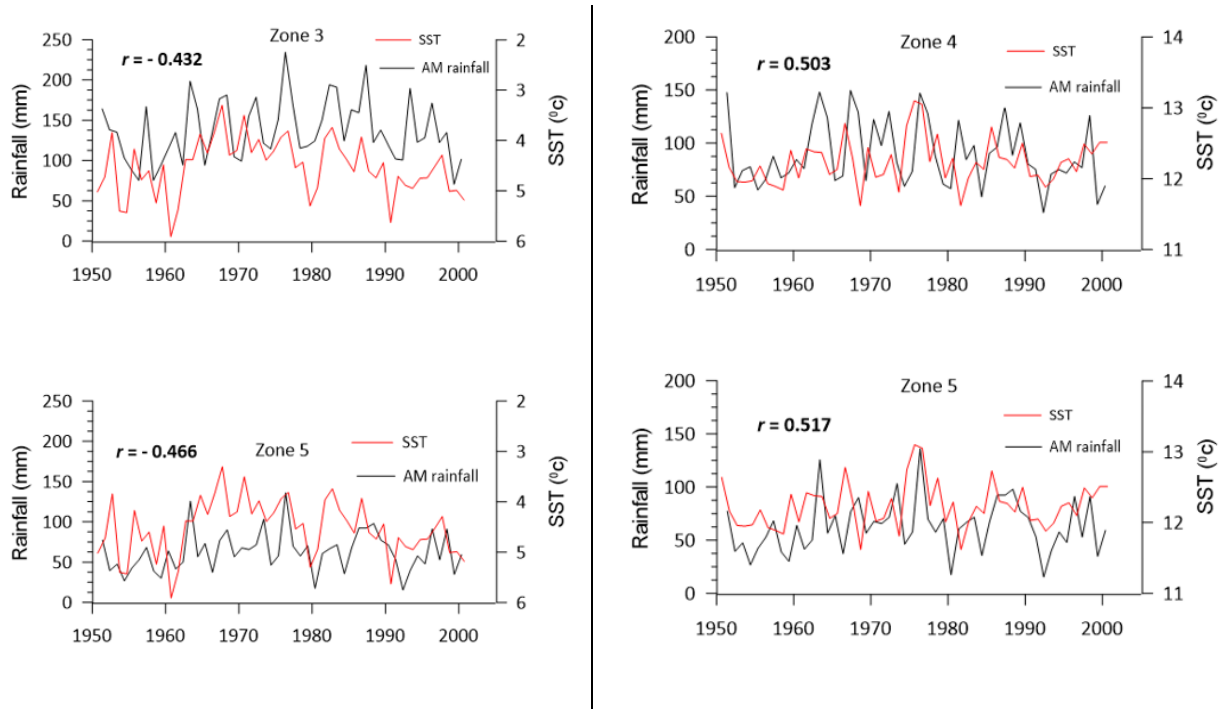

Figure 3.11 Significant cross-correlations between selected spring rainfall zones and oceanic SSTs at lag times of 6–7 months for zones 3 & 5 (left side) and 7–8 months for zones 4 & 5 (right side) for the rainfall time series (1951–2000).

3.4. Conclusions

Ethiopian rainfall is characterized by both seasonal and interannual spatial variabilities. Thus, understanding the teleconnection (remote link) between Ethiopian rainfall and oceanic SSTs is a key factor for establishing future rainfall prediction models and further managing the country's water resources.

For this reason, this study was directed toward analyzing rainfall time series on both seasonal and annual scales, investigating their potential trends, and detecting their significance over Ethiopia, along with investigating the oceanic SST regions that significantly influence Ethiopian rainfall in order to detect the potential SST regions that could be valuable as input data for establishing forecasting models in further studies.

Firstly, in this study, rainfall data for summer (1951–2015) and spring (1951–2000) seasons were analyzed for identification of the rainfall peaks of July/August and April/May for summer and spring seasons, respectively.

Secondly, preliminary clustering or dividing of Ethiopia into homogenous rainfall zones was applied, depending on seasonality and spatial homogeneity of rainfall data, which introduced a new number of rainfall zones for Ethiopia with 14 homogenous rainfall zones: nine rainfall zones for summer peak July/August and five zones for spring peak April/May.

Thirdly, cross-correlations between SST and rainfall peaks at the 0.01 significance level revealed oceanic regions that significantly influence rainfall over Ethiopia at different lag times. For summer rainfall (main rainy season), the influence of Gulf of Guinea (positive correlation) and two regions in the southern Pacific Ocean (positive and negative correlations) was significantly detected at a lag time of 5–6 months.

In addition, SST of northwestern Pacific showed a weak negative influence on summer northern rainfall zones (1 and 2) at a lag time 7–8 months, whereas SST of the Indian Ocean indicated a significantly negative effect on summer eastern and western zones (5 and 7) at a lag time of 6–7 months, being close to Ethiopia. For spring rainfall, the negative influence of the northern Atlantic Ocean SST was strongly detected on spring rainfall zones (3 and 5) at a lag time of 6–7 months, whereas two areas of the Indian Ocean showed a positive correlation between SSTs and spring rainfall zones (4 and 5).

Finally, correlation coefficients (r) between these significant SST oceanic regions and both summer and spring rainfalls were derived for detection of the SST regions that could be valuable as input data for prediction models at lead times before both seasons. For the summer season, at a lag time of 5–6 months, both central zones (8 and 9) exhibited the strongest positive correlation ($r \geq 0.46$) between summer rainfall and southern Pacific Ocean SST, among all other summer zones

due to the difference between positive and negative correlations at the two areas of the southern Pacific Ocean. Alternatively, a significantly negative correlation ($r \geq -0.40$) was identified between spring rainfall zones (3 and 5) and the northern Atlantic Ocean SST at a lag time of 6–7 months before spring season.

Therefore, for later studies, it is recommended to use SST regions of the southern Pacific and northern Atlantic oceans as effective input data for forecasting models of Ethiopian summer and spring rainfall peaks at lead times of 5–6 and 6–7 months, respectively.

Chapter 4

General Conclusions and recommendations

4.1. General conclusions

For Lake Tana basin (local-scale), the results indicated that the rainfall pattern over the basin is a monomodal with a rainfall peak in July/August. Moreover, the annual rainfall trend tends to alternate between dry and wet. The normalization of the selected long-term of rainfall data from 1985 to 2015 (65 years of rain data). Mostly, the change in the annual rainfall data over time is not statistically significant. The Blue Nile basin is the only surface water outflow of Lake Tana basin, the latter is the largest fresh water source for the Blue Nile River and consequently, for the River Nile as a main water source for Sudan and Egypt. The basin is characterized by high spatial rainfall variability. Therefore, Oceanic SST to rainfall teleconnection is challenging.

The results of cross-correlations between summer rainfall data (June-September) and climatic indices showed a positive correlation with AO, MOI, and SOI indices, while the PDO has a significant negative correlation with summer rains at lags 0-9 months. Such results indicate the major influence of Pacific SST on summer rainfall at the basin. The two-tailed with 0.05 significance level was adopted in this study. The correlation was applied at a significance level of 0.05 at lag time from 0 to 9 months before the summer rainy season (JJAS).

Essentially, the results of teleconnections of SST-rainfall were significant at a lead time of 4-5 months prior the rainy season (JJAS) meaning that January- February monthly SST data were linked to summer rains over the basin. Two regions of the Pacific Ocean indicated a significant correlation, one area near Philippines where the SST was positively correlated with summer rainfall of about 0.63. The other area off the northern coast of America showed a significant negative correlation with rainfall of about -0.54.

These significant teleconnections between two regions of Pacific SST and rainfall were used as input data for constructing the prediction model for the long-term rainfall data over the basin

(65 years). The artificial Elman recurrent neural network enhanced the results of correlation between Pacific SSTs and summer rains to 0.8 and 0.7 of correlations between summer rainfall between and oceanic SST regions of western Pacific and north eastern Pacific, respectively.

Generally, the results of this study indicate that neural network model could be skillful enough for seasonal rainfall prediction over the basin that would beneficial for more precise water allocation among downstream countries (Egypt and Sudan) and for early warnings of the hydrological extremes as flood or drought. The study recommends to apply neural network prediction model on large-scale, i.e. Ethiopia as a whole taking into consideration the various variations in meteorological properties over the country from one region to another.

The results of statistical analysis of rainfall variability over all of Ethiopia (large-scale study) indicated that the rainfall trends have a bimodal trend for both summer (April and July/August) and spring rains (April/May and October). Where, two peaks for rainfall in Ethiopia were identified, which are July/August for summer rainy season and April/May for spring season. For Summer rains (JJAS), the results of the standardization of rainfall changes over the selected long-term period (1950-2015) indicated a statistically significant interdecadal rainfall variability over time with some drought events recorded in 1965, 1984, and 2002. For spring rains (1950-2000), a statistically prominent interdecadal rainfall variability occurs over time with 5 periods of drought events in 1952, 1965, 1974, 1980, and 1984.

Dividing Ethiopia into homogenous rainfall zones is a crucial factor due to the high spatial variability of seasonal and annual rainfall from one area to another. The outcomes of this regionalization result in dividing Ethiopia into 9 zones for summer rainfall and 5 zones for spring rainfall. At a significance level of 0.01, the result of cross-correlations shows significant teleconnections between summer rainfall and Oceanic SSTs of Indian, Pacific, Oceans and Gulf

of Guinea at a lag time of 5-7 months. While, the spring rainfall peaks has a significant correlation with Oceanic SST regions of northern Atlantic and Indian Oceans.

Further results detected certain oceanic SST regions the significantly influenced rain peaks in summer and spring seasons. These regions would be useful as input data for further prediction models over Ethiopia. For instance, the study investigated that the central summer rainfall zones (8 and 9), of all 9 summer zones of rainfall, are strongly correlated with SST of southern Pacific Ocean at a lag time of 5-6 months. Moreover, the spring rainfall zones (3 and 5) show a significant correlation with SST of northern Atlantic Ocean at lag time of 6-7 months. Generally, this study focused on the first rainy season (FMAM) and the second rainy season (JJAS) over Ethiopia and addressed the significant influence of SSTs of northern Atlantic and southern Pacific Oceans on spring and summer rainfall zones, respectively.

4.2. Recommendations

Based on this research study, the author recommends the following:

- The government should provide more advanced technology to observe rainfall over the country, as the quality of results relies on the quality of rainfall data.
- Specifically, further research studies are required to investigate the influence of oceanic SSTs on rainfall variability over southern part of Ethiopia, especially for the main rainfall season from March to May (MAM) and for the secondary rainfall season ranging from September to November (SON).
- Essentially, more studies on both scales (local and large) over Ethiopia are required to improve the assessment of spatio-temporal rainfall variations related to SST. Therefore, it would be beneficial for enhancing the prediction ability of rainfall over the country. Consequently, more benefits for water source management and socio-economic aspects.

References

Abegaz A, Keulen H, Haile M, Oosting S (2007) Nutrient dynamics on smallholder farms in Teghane, northern High- lands of Ethiopia. Advances in Integrated Soil Fertility Man- agement in Sub-Saharan Africa: Challenges and Opportunities, A. Bationo et al., Eds., Springer, 365–378.

Abeje MT, Tsunekawa A, Haregeweyn N, Nigussie Z, Adgo E, Ayalew Z, Tsubo M, Elias A, Berihun D, Quandt A, Berihun ML (2019) Communities' Livelihood Vulnerability to Climate Variability in Ethiopia. Sustainability 11 (22), p. 6302.

Abtew W, Melesse AM, Dessalegne T (2009) El Niño southern oscillation link to the Blue Nile River basin hydrology. Hydrol Process 23: 3653–3660.

Abtew W, Melesse AM (2014) The Nile River Basin. In: Mesele AM, Abtew W, Setegn S (Eds) Nile River basin: Ecohydrological challenges, climate change and hydropolitics, pp: 7–17, Springer-Verlag.

Alemayehu T, McCartney M, Kebede S (2009) Simulation of water resource development and environmental flows in the Lake Tana Subbasin. In: S. B. Awulachew, T. Erkossa, V. Smakhtin & A. Fernando (eds). Improved Water and Land Management in the Ethiopian Highlands: Its Impact on Downstream Stakeholders Dependent on the Blue Nile. Intermediate Results Dissemination Workshop held at the International Livestock Research Institute (ILRI), Addis Ababa, Ethiopia, 5–6 February 2009. International Water Management Institute, Colombo, Sri Lanka, pp. 23–37.

Alexandersson H, Moberg A (1997) Homogenization of Swedish temperature data. Part I: Homogeneity test for lineal trends. Int. J. Climatol. 17: 25–34.

Alhamshry A, Fenta AA, Yasuda H, Shimizu K, Kawai T (2019) Prediction of summer rainfall over the source region of the Blue Nile by using teleconnections based on sea surface temperatures. Theor. Appl. Climatol 137(3-4), pp: 3077-3087.

Amarasekera K, Lee R, Williams E, Eltahir E (1997) ENSO and the natural variability in the flow of tropical rivers. J Hydrol 200 (1–4): 24–39.

Anderson RL (1942) Distribution of the serial correlation coefficient. Ann. Math. Stat. 13: 1–13.

Asnani G (2005) Tropical Meteorology, revised ed.; Praveen Printing Press: Puna, India, Vol.1.

Awlachew SB (2010) Irrigation potential in Ethiopia. International Water Management Institute, Addis Ababa, Ethiopia.

Baigorria GA, Jones JW, O'Brien JJ (2007) Understanding rainfall spatial variability in southeast USA at different timescales. Int. J. Climatol. 27: 749–760.

Barnes J (2017) The future of the Nile: climate change, land use, infrastructure management, and treaty negotiations in a transboundary river basin. WIREs Clim Change e449.

Barrow CJ (1992) World atlas of desertification (United Nations Environment Programme). Land Degrad Dev 3(4): 249–249.

Bekele F (1997) Ethiopian use of ENSO information in its seasonal forcasts. Int. J. Afr. Stud. Volume 2.

Belay AS, Fenta AA, Yenehun A, Nigate F, Tilahun SA, Moges MM, Dessie M, Adgo E, Nyssen J, Chen M, Griensven AV (2019) Evaluation and Application of Multi-Source Satellite Rainfall Product CHIRPS to Assess Spatio-Temporal Rainfall Variability on Data-Sparse Western Margins of Ethiopian Highlands. Remote Sens. 11 (22), p. 2688.

Beltrando G, Camberlin P (1993) Interannual variability of rainfall in the eastern Horn of Africa and indicators of atmospheric circulations. Int J Climatol 13: 533–546.

Berhanu B, Seleshi Y, Melesse AM (2014) Surface water and groundwater resources of Ethiopia: Potentials and challenges of water resources development. In: Mesele AM, Abtew W, Setegn S (Eds) Nile River basin: Ecohydrological challenges, climate change and hydropolitics, pp: 97–117, Springer-Verlag.

Berhane F, Zaitchik B, Dezfuli A (2014) Subseasonal analysis of precipitation variability in the Blue Nile River Basin. J Clim 27(1): 325–344.

Berihun ML, Tsunekawa A, Haregeweyn N, Meshesha DT, Adgo E, Tsubo M, Masunaga T, Fenta AA, Sultan D, Yibeltal M, Ebabu K (2019) Hydrological responses to land use/land cover change and climate variability in contrasting agro-ecological environments of the Upper Blue Nile basin, Ethiopia. Sci. Total Environ. 689: 347–365.

Bishop CM (1995) Neural Networks for pattern recognition. Oxford University Press, New York.

Block P, Rajagopalan B (2007) Interannual variability and ensemble forecast of Upper Blue Nile Basin Kiremt season precipitation. J. Hydrometeorol. 8: 327–343.

Box GEP, Jenkins GM, Reinsel GC, Ljung GM (1970) Time Series Analysis, Forecasting and Control, 5th ed.; Holden-Day: San Francisco, CA, USA. ISBN 978-1-118-67502-1.

Brown DP, Comrie AC (2004) A winter precipitation ‘‘dipole’’ in the western United States associated with multi-decadal ENSO variability. Geophys Res Lett 31: L09203.

Camberlin P (1995) June–September rainfall in north-eastern Africa and atmospheric signals over the tropics: A zonal perspective. Int J Clim 15: 773–783.

Camberlin P (1997) Rainfall anomalies in the source region of the Nile and their connection with the Indian summer monsoon. J Clim 10(6): 1380–1392.

Camberlin P, Janicot S, Poccard I (2001) Seasonality and atmospheric dynamics of the teleconnection between African rainfall and tropical sea surface temperature: Atlantic vs. ENSO. Int. J. Climatol. 21: 973–1005.

Camberlin P, Fontaine B, Louvet S, Oettli P, Valimba P (2010) Climate adjustments over Africa accompanying the Indian monsoon onset. J Clim 23: 2047–2064.

Cheung WH, Senay GB, Singh A (2008) Trends and spatial distribution of annual and seasonal rainfall in Ethiopia. Int. J. Climatol. 28: 1723–1734.

Cho V (2003) A comparison of three different approaches to tourist arrival forecasting. Tourism Management 24 (2003): 323-330.

Conway D (2000) The climate and hydrology of the Upper Blue Nile River. Geogr J 166(1): 49–62.

Dash NB, Panda SN, Remesan R, Sahoo N (2010) Hybrid neural modeling for groundwater level prediction. Neural Compt Appl 19(8): 1251-1263.

Degefu W (1987) Some aspects of meteorological drought in Ethiopia. Drought and Hunger in Africa: Denying Famine a Future, M. H. Glantz, Ed., Cambridge University Press, 23–36.

Degefu MA, Rowell DP, Bewket W (2017) Teleconnections between Ethiopian rainfall variability and global SSTs: Observations and methods for model evaluation. Meteorol. Atmos. Phys. 129: 173–186.

Deser C, Phillips AS, Alexander MA (2010) Twentieth century tropical sea surface temperatures trends revisited. Geophys Res Lett 37: L10701.

Digna R, Castro-Gama M, van der Zaag P, Mohamed Y, Corzo G, Uhlenbrook S (2018) Optimal operation of the Eastern Nile System using Genetic Algorithm, and benefits distribution of water resources development. Water 10 (7): p. 921.

Dinku T, Funk C, Peterson P et al (2018) Validation of CHIRPS satellite rainfall estimates over Eastern of Africa. Q J Royal Meteorol Soc 144: 292-312.

Diro GT, Black E, Grimes DIF (2008) Seasonal forecasting of Ethiopian spring rains. Meteorol. Appl. 15: 73–83.

Diro GT, Grimes DIF, Black E, O'Neill A, Pardo-Iguzquiza E (2009) Evaluation of reanalysis rainfall estimates over Ethiopia. Int. J. Climatol. 29: 67–78.

Diro GT, Grimes DIF, Black E (2011a) Teleconnections between Ethiopian summer rainfall and sea surface temperature: Part I. Observation and modeling. Clim Dyn 37(1): 121–131.

Diro GT, Grimes DIF, Black E (2011b) Teleconnections between Ethiopian summer rainfall and sea surface temperature: Part II. Seasonal forecasting. Clim Dyn 37(1): 121–131.

Dyer T (1975) The assignment of rainfall stations into homogeneous groups: An application of principal component analysis. Q. J. R. Meteorol. Soc. 101: 1005–1013.

Ebabu K, Tsunekawa A, Haregeweyn N et al (2018) Analyzing the variability of sediment yield: a case study from paired watersheds in the Upper Blue Nile basin, Ethiopia. Geomorphology 303: 446–455.

Ebabu K, Tsunekawa A, Haregeweyn N, Adgo E, Meshesha DT, Aklog D, Masunaga T, Tsubo M, Sultan D, Fenta AA, Yibeltal M (2019) Effects of land use and sustainable land management practices on runoff and soil loss in the Upper Blue Nile basin, Ethiopia. Sci. Total Environ. 648:1462–1475.

Ehrendorfer MA (1987) regionalization of Austria's precipitation climate using principal component analysis. J. Clim. 7: 71–89.

Elman JL (1990) Finding Structure in Time. Cognitive Sci 14: 179-21.

Elsanabary MH, Gan TY (2014) Wavelet analysis of seasonal rainfall variability of the Upper Blue Nile Basin, its teleconnection to global sea surface temperature, and its forecasting by an Artificial Neural Network. MonWea Rev 142(5): 1771–1791.

FAO (Food and Agriculture Organization) (2016) AQUASTAT Ethiopia: http://www.fao.org/nr/water/aquastat/countries_regions/ETH/, accessed February 22, 2018.

Fazzini M, Bisci C, Billi P (2015) The Climate of Ethiopia. In: Billi P (ed) Landscapes and Landforms of Ethiopia, pp. 65–87, Springer-Verlag.

Fenta AA, Yasuda H, Shimizu K, Haregeweyn N, Kawai T, et al (2017a). Spatial distribution and temporal trends of rainfall and erosivity in the Eastern Africa region. Hydrol Process 31(25): 4555–4567.

Fenta AA, Kifle A, Gebreyohannes T, Hailu G (2015) Spatial analysis of groundwater potential using remote sensing and GIS-based multi-criteria evaluation in Raya Valley, northern Ethiopia. Hydrogeol. J. 23 (1): 195–206.

Fenta AA, Yasuda H, Shimizu K, Haregeweyn N, Negussie A (2016) Dynamics of soil erosion as influenced by watershed management practices: a case study of the Agula watershed in the semi-arid highlands of northern Ethiopia. Environ Manag 58: 889–905.

Fenta AA, Yasuda H, Shimizu K, Haregeweyn N (2017a) Response of streamflow to climate variability and changes in human activities in the semi-arid highlands of northern Ethiopia. Reg Environ Change 17:1229–1240.

Fenta AA, Yasuda H, Shimizu K, Haregeweyn N, Kawai T, Sultan D, Ebabu K, Belay AS (2017b) Spatial distribution and temporal trends of rainfall and erosivity in the Eastern Africa region. Hydrol Process 31: 4555-4567.

Fenta AA, Yasuda H, Shimizu K, Haregeweyn N, Woldearegay K (2017b) Quantitative analysis and implications of drainage morphometry of the Agula watershed in the semi-arid northern Ethiopia. Appl. Water Sci. 7 (7): 3825–3840.

Fenta AA, Yasuda H, Shimizu K, Ibaraki Y, Haregeweyn N, Kawai T, Belay AS, Sultan D, Ebabu K (2018) Evaluation of satellite rainfall estimates over the Lake Tana basin at the source region of the Blue Nile River. Atmos Res 212: 43-53.

Fenta AA (2018) Effect of watershed management practices on hydrological response and soil erosion in the semiarid highlands of northern Ethiopia (Doctoral thesis). https://repository.lib.tottori-u.ac.jp/6269. Accessed on April 2020.

Fenta AA, Tsunekawa A, Haregeweyn N, Poesen J, Tsubo M, Borrelli P, Panagos P, Vanmaercke M, Broeckx J, Yasuda H, Kawai T (2019) Land susceptibility to water and wind erosion risks in the East Africa region. Sci. Total Environ. 703, 135016.

Folland C, Palmer T, Parker D (1986) Sahel rainfall and worldwide sea temperatures 1901–1985. Nature 320: 602–607.

Funk C, Peterson P, Landsfeld M et al (2015) The climate hazards infrared precipitation with stations - A new environmental record for monitoring extremes. Sci Data 2: 1–21.

Gadgil S, Josh NV (1993) Coherent rainfall zones of the Indian region. Int. J. Clim. 13: 547–566.

Gamachu D (1977) Aspects of Climate and Water Budget in Ethiopia. Addis Ababa University Press, pp 71.

Gamachu D (1988) Some patterns of altitudinal variation of climatic elements in the mountainous regions of Ethiopia. Mt. Res. Dev 8: 131–138.

Gebrehiwot T, van der Veen A, Maathuis B (2011) Spatial and temporal assessment of drought in the northern highlands of Ethiopia. Int J Appl Earth Obs Geoinf 13: 309–321.

Gebremedhin MA, Abraha AZ, Fenta AA (2017) Changes in future climate indices using Statistical Downscaling Model in the upper Baro basin of Ethiopia. Theor Appl Climatol 133: 39-46.

Gershunov A, Barnett TP (1998) Interdecadal modulation of ENSO teleconnections. Bull Amer Meteor Soc 79: 2715–2725.

Ghosh S, Luniya V, Gupta A (2009) Trend analysis of Indian summer monsoon rainfall at different spatial scales. Atmos. Sci. Lett. 10: 285–290.

Gissila T, Black E, Grimes DIF, Slingo JM (2004) Seasonal forecasting of the Ethiopian summer rains. Int J Climatol 24: 1345–1358.

Gleixner S, Keenlyside N, Viste E, Korecha D (2017a) The El Niño effect on Ethiopian summer rainfall. Clim Dyn49(5–6): 1865–1883.

Gleixner S, Keenlyside NS, Demissie TD et al (2017b) Seasonal predictability of Kiremt rainfall in coupled general circulation models. Environ Res Lett 12: 114016.

Goyal MK, Ojha CSP (2012) Downscaling of surface temperature for lake catchment in an arid region in India using linear multiple regression and neural networks. Int J Clim 32: 552–566.

Griffiths J (1972) Ethiopian Highlands. In Climates of Africa, World Survey of Climatology, 2nd ed.; Elsevier: Amsterdam, The Netherlands, Volume 10, pp. 369–388.

Haregeweyn N, Tsunekawa A, Poesen J et al (2017) Comprehensive assessment of soil erosion risk for better land use planning in river basins: Case study of the Upper Blue Nile River. Sci Total Environ 574:95–108.

Hirsch RM, Helsel DR, Cohn TA, Gil EJ (1993) Statistical analysis of hydrologic data. In Handbook of Hydrology; Maidment, D.R., Ed.; McGraw-Hill: New York, NY, USA, Volume 17, pp. 11–37.

Hu ZZ, Huang B (2009) Interferential impact of ENSO and PDO on dry and wet conditions in the U.S. Great Plains J Clim 22: 6047–6065.

Indeje M, Semazzi FH, Ogallo LJ (2000) ENSO signals in East African rainfall seasons. Int J Clim 20: 19–46.

Jury MR (2010) Ethiopian decadal climate variability. Theor Appl Clim 101: 29–40.

Jury MR, Funk C (2012) Climatic trends over Ethiopia: Regional signals and drivers. Int. J. Climatol 33: 1924–1935.

Kassahun B (1987) Weather Systems over Ethiopia. In Proceedings of the First Technical Conference on Meteorological Research in Eastern and Southern Africa, Kenya Meteorological Department, Nairobi, Kenya. January 6, pp.53-57.

Kebede S, Travi Y, Alemayehu T et al (2006) Water balance of Lake Tana and its sensitivity to fluctuations in rainfall, Blue Nile basin, Ethiopia. J Hydro 316: 233–247.

Kendall MG, Stuart A (1948) The Advanced Theory of Statistics, 4th ed.; Charles Griffin: London, UK.

Kloos H, Legesse W (2010) Water Resources Management in Ethiopia: Implications for the Nile Basin. Cambria Press, pp 444.

Kodera K (2004) Solar influence on the Indian Ocean Monsoon through dynamical processes. Geophys. Res. Lett. 31, 24.

Korecha D, Barnston AG (2007) Predictability of June–September rainfall in Ethiopia. Mon Wea Rev135(2): 628–650.

Korecha D, Sorteberg A (2013) Validation of operational seasonal rainfall forecast in Ethiopia. Water Resour. Res. 49: 7681–7697.

Kumbuyo C, Yasuda H, Kitamura Y, Shimizu K (2014) Fluctuation of rainfall time series in Malawi: An analysis of selected areas. Geofizika 31:13-34.

Kurtzman D, Scanlon BR (2007) El Niño–Southern Oscil-lation andPacific decadal oscillation impacts on precipitation in the southern and central United States: Evaluation of spatial distribution and predictions. Water Resour Res 43: W10427.

Lamb HF, Bates CR, Coombes PV, Marschall MH, Umer M, Davies SJ, Dejen E (2007) Late Pleistocene dessication of Lake Tana, source of the Blue Nile. Quaternary Research 26: 287–299.

Lin H, Brunet G, Derome J (2009) An Observed Connection between the North Atlantic Oscillation and the Madden–Julian Oscillation. J Climate 22(2): 364–380.

Lloyd-Hughes B, Saunders MA (2002) Seasonal prediction of European spring precipitation from El Nino Southern Oscillation and local sea-surface temperatures. Int J Clim 22 (1): 1-14.

Lucio PS, Molion LCB, de Avila Valadão C, Conde FC, Ramos AM, de Melo MLD (2012) Dynamical outlines of the rainfall variability and the ITCZ role over the West Sahel. Atmos. Clim. Sci. 2 (3): 337–350.

Lyon B (2014) Seasonal drought in the Greater Horn of Africa and its recent increase during the March-May long rains. J Clim 27(21): 7953–7975.

Mair A, Fares A (2010) Assessing rainfall data homogeneity and estimating missing records in Mākaha Valley, O'ahu Hawai'i. J. Hydrol. Eng. 15: 101–106.

Mantua NJ, Hare SR, Zhang Y, Wallace JM, Francis RC (1997) A Pacific interdecadal climate oscillation with impacts on salmon production. Bull Amer Meteor Soc 78: 1069–1080.

McCabe GJ, Ault TR, Cook BI, Betancourt JL, Schwartz MD (2012) Influences of the El Niño Southern Oscillation and the Pacific decadal oscillation on the timing of the North Ameri-can spring. Int J Climatol 32:2301–2310.

McCartney M, Alemayehu T, Shiferaw A, Awulachew, SB (2010) Evaluation of current and future water resources development in the Lake Tana Basin, Ethiopia. Int Water Management Institute, Colombo, Sri Lanka 44 pp. ISBN 978-92-9090-721-3.

McCuen RH (2003) Modeling Hydraulic Change: Statistical Methods; Lewis: Boca Raton, FL, USA, pp. 16–36, ISBN 978-1-4200-3219-2.

McHugh MJ, Rogers JC, McHugh MJ, Rogers JC (2001) North Atlantic Oscillation Influence on Precipitation Variability around the Southeast African Convergence Zone. J Climate 14(17): 3631–3642.

Mohr PA, (1962) The Geology of Ethiopia. Addis Ababa, Ethiopia. University College of Addis Ababa Press.

Nicholson SE (2017) Climate and climatic variability of rainfall over eastern Africa. Reviews of Geophys 55(3): 590–635.

Oakley NS, Redmond KT (2014) Aclimatology of 500-hPa closed lows in the northeastern Pacific Ocean, 1948–2011. J Appl Meteor Climatol 53:1578–1592.

Olsson J, Uvo CB, Jinno K (2001) Statistical atmospheric downscaling of short–term extreme rainfall by neural networks. Phys Chem Earth Pt B 26:695–700.

Rajeevan M, Bhate J, Kale JD, Lal B (2006) High resolution daily gridded rainfall data for the Indian region: Analysis of break and active monsoon spells. Curr. Sci. 91: 296–306.

Rayner N, Parker D, Horton E, et al (2003) Global analysis of Sea surface temperature, sea ice and night marine air temperature since the late nineteenth century. J Geophys Res 108(d14).

Rzóska J, (1976a) Lake Tana, headwaters of the Blue Nile. In J. Rzóska (ed.), The Nile, Biology of an Ancient River. Junk, The Hague, pp. 223–232.

Saji NH, Goswami BN, Vinayachandran PN, Yamagata T (1999) A dipole mode in the tropical Indian Ocean. Nature 401: 360–363.

Segele ZT, Lamb PJ (2005) Characterization and variability of Kiremt rainy season over Ethiopia. Meteorol Atmos Phys 89:153–8.

Segele ZT, Lamb PJ, Leslie LM (2009a) Large-scale atmospheric circulation and global sea surface temperature associations with Horn of Africa June–September rainfall. Int J Climatol 29:1075–100.

Segele Z, Lamb PJ, Leslie LM (2009b) Seasonal-to-interannual variability of Ethiopia/Horn of Africa monsoon. Part I: Associations of Wavelet-Filtered large-scale atmospheric circulation and global sea surface temperature. J. Clim. 22: 3396–3421.

Seleshi Y, Demaree GR (1995) Rainfall variability in the Ethiopian and Eritrean highlands and its links with the Southern Oscilation Index. J Biogeogr 22: 945–952.

Seleshi Y, Zanke U (2004) Recent changes in rainfall and rainy days in Ethiopia. J Climatol 24:973–983.

Setegn SG, Srinivasan R, Dargahi B (2008) Hydrological modelling in the Lake Tana Basin, Ethiopia using SWAT model. Open Hydrol. J. 2 (1): 49–62.

Sfersos A, Coonick AH (2000) Univariate and multivaiate forecasting of hourly solar radiatin with artificial intelligence techniques. Solar Energy 68: 169–178.

Shahin M, (1985) Hydrology of the Nile Basin. Elsevier, 575 pp. Sutcliffe, J. V., and Y. P. Parks, 1999: The Hydrology of the Nile. IAHS Special Publ. 5, pp179.

Smith IN, McIntosh P, Ansell TJ, Reason CJC, McInnes K (2000) Southwest western Australian winter rainfall and its association with ocean climate variability. Int J Climatol 20:1913–1930.

Sultan D, Tsunekawa A, Haregeweyn N et al (2018a) Impact of soil and water conservation interventions on watershed runoff response in a tropical humid highland of Ethiopia. Environ Manag 61: 860–874.

Sultan D, Tsunekawa A, Haregeweyn N et al (2018b) Efficiency of soil and water conservation practices in different agro-ecological environments of Ethiopia's Upper Blue Nile basin. J Arid Land 10(2): 249–263.

Sutcliffe JV, Parks YP (1999) The Hydrology of the Nile. IAHS Special Publ. 5, 179 pp.

Taye MT, Willems P (2012) Temporal variability of hydroclimatic extremes in the Blue Nile basin. Water Resour Res 48 (3):1–13.

Tegegne G, Hailu D, Aranganathan SM (2013) Lake Tana reservoir water balance model. Int. J. Appl. Innov. Eng. Manage. (IJAIEM) 2 (3): 474–478.

Tootle GA, Piechota TC (2006) Relationships between Pacific and Atlantic Ocean sea surface temperatures and US streamflow variability. Water Resour. Res. 42, W07411.

Tsidu GM (2012) High-resolution monthly rainfall database for Ethiopia: Homogenization, reconstruction, and gridding. J. Clim. 25: 8422–8443.

UNESCO (United Nations Educational, Scientific, and Cultural Organization) (2004) National Water Development Report for Ethiopia (Final). Addis Ababa, Ethiopia.

Uvo CB, Repelli CA, Zebiak SE, Kushnir Y (1998) The relationships between tropical Pacific and Atlantic SST and northeast Brazil monthly precipitation. J Clim 11: 551–562.

Verdin J, Funk C, Senay G, Choularton R (2005) Climate scienceand famine early warning. Philos. Trans. R. Soc. B Biol. Sci. 360: 2155–2168.

Viste E, Sorteberg A (2013) Moisture transport into the Ethiopian highlands. Int J Climatol 33: 249–263.

Wagesho N, Goel NK, Jain MK (2013) Temporal and spatial variability of annual and seasonal rainfall over Ethiopia. Hydrol. Sci. J. 58: 354–373.

Wang D, Wang C, Yang X, Lu J (2005) Winter Northern Hemisphere surface air temperature variability associated with the Arctic Oscillation and North Atlantic Oscillation. Geophys Res Lett 32(16): L16706.

Williams AP, Funk C, Michaelsen J et al. (2012) Recent summer precipitation trends in the Greater Horn of Africa and the emerging role of Indian Ocean sea surface temperature. Clim Dyn 39: 2307–2328.

Wolde-Georgis T, Aweke D, Hagos Y (2001) The case of Ethiopia: Reducing the impacts of environmental emergen- cies through early warning and preparedness: The case of the 1997–98 El Ni~no. United Nations University, 73 pp. [Available online at archive.unu.edu/env/govern/ElNIno/CountryReports/ pdf/ethiopia.pdf.]

Woldesenbet TA, Elagib NA, Ribbe L, Heinrich J (3018) Catchment response to climate and land use changes in the Upper Blue Nile sub-basins, Ethiopia. Sci. Total Environ. 644: 193–206.

Yasuda H, Berndtsson R, Saito T, Anyoji H, Zhang X (2009) Prediction of Chinese Loess Plateau summer rainfall using Pacific Ocean spring sea surface temperature. Hydrol Process 23: 719–729.

Yasuda H, Nandintsetseg B, Berndtsson R, Shinoda M, Kawai T (2017) The Effects of Ocean SST Dipole Differences on Mongolian Summer Rainfall. Geofizika.

Yasuda H, Panda SN, Abd Elbasit MAM, Kawai T, Elgamri T, Fenta AA, Nawata H (2018) Teleconnection of rainfall time series in the central Nile Basin with sea surface temperature. Paddy and Water Environment (0123456789).

Yates DN, Strzepek KM (1998) Modeling the Nile basin under climatic change. J. Hydrol. Eng. 3: 98–108.

Yuan F, Yasuda H, Berndtsson R, Uvo CB, Zhang L, Hao Z, Wang XP (2016) Regional sea surface temperatures explain spatial and temporal variation of summer rainfall in the source region of the Yellow River. Hydrol Sci J. 61: 1383-1394.

Zaroug MAH, Eltahir EAB, Giorgi F (2014) Droughts and floods over the upper catchment of the Blue Nile and their connections to the timing of El Niño and La Niña events. Hydrol. Earth Syst. Sci. 18: 1239–1249.

Zaroug MAH, Giorgi F, Coppola E, Abdo GM, Eltahir EAB (2014) Simulating the connections of ENSO and the rainfall regime of East Africa and the upper Blue Nile region using a climate model of the Tropics. Hydrol. Earth Syst. Sci. 18: 4311–4323.

Zhang X, Wang J, Zwiers FW, Groisman PY (2010) The influence of large-scale climate variability on winter maximum daily precipitation over North America. J Clim 23: 2902–2915.

Zhang Y, Moges S, Block P (2016) Optimal cluster analysis for objective regionalization of seasonal precipitation in regions of high spatial–temporal variability: Application to Western Ethiopia. J. Clim. 29: 3697–3717.

Summary

The rainfall variability across time and space influences all aspects of human activities, especially socio-economic ones. Particularly, the rainfall over Ethiopia is characterized by high spatial and temporal variations due to complex topography (highlands and lowlands) and geographical location. The rainfall is considered to be the most crucial meteorological parameter in Ethiopia. Thus, these spatio-temporal variations are required to be fully investigated for many reasons; agriculture in Ethiopia is the major sector that mainly depends on rainfall with about 85% of labor force in the country, as well as the rainfall is vital for hydro power projects that accounts for about 98% of the energy production.

One of the large-scale drivers affect rainfall over Ethiopia is Sea Surface Temperature (SST) and could be used as a key predictor that slowly changed. Three main seasons of rainfall over the country; summer rainy (June-September), winter dry (October-January), and spring mid-rainy (February-May) seasons. Most of the previous studies focused only on the main summer rainy season, while the spring rainfall was investigated in a few numbers of researches. Therefore, the main objective of this study is to present more investigation for spring rainfall, as well as summer rains over both local and large scales. Moreover, this study aims to improve our understanding for the teleconnection between SST and rainfall over Ethiopia.

No doubt, the full investigation for this relationship will enhance the quality and accuracy of rainfall prediction models. Consequently, such accurate models would be beneficial for water sources management, development plans, addressing the hydrological extremes (flood and drought), and water allocation between Ethiopia and its downstream neighbors (Sudan and Egypt).

The first study focused on the statistical analysis of summer rainfall data (1985-2015) on a local-scale over Lake Tana. The latter is the main freshwater source for the Blue Nile River which contributes to about 60% of the Nile River flow. In addition, investigating the teleconnection between oceanic SSTs and summer rains over and counter and finally using the Artificial Neural Network (ANN) model for summer rainfall prediction over the basin.

The summer rains over the basin extend from June to September (JJAS that is locally known as Kiremt). The basin was considered as one single area, where the results indicated that summer rains have a monomodal trend with a high peak in July/August. The interannual rainfall variability alternates between wet and dry with no significant change over time. The cross-correlation at a significance level of 0.05, indicated a significant teleconnection between oceanic SST and summer rains at a lead time of 4-5 months prior to the rainy season. Especially, two SST regions in the Pacific Ocean had such an impact on rainfall.

Furthermore, these tele-connected areas were used as input data for prediction model of ANN. The final result showed that the ANN model would be skillful enough for enhancing rainfall prediction over the basin, as it enhanced the correlation between summer rainfall and SST data for about 0.8.

The second study aimed to expand the investigation about the influence of SST on rainfall from basin local size (Lake Tana) to the countrywide (Ethiopia). Moreover, both summer and spring rainy seasons were addressed. The long-term data for 65 years of summer rains and 50 years of spring rainfall were used. The results indicated the bimodal rainfall trend over the country with two peaks in July/August and April/May for summer and spring seasons, respectively.

The regionalization of the country was crucial due to high spatio-temporal interdecadal rainfall variability. Ethiopia was divided into 14 rainfall zones in this study, 9 summer zones and 5 spring zones. The results of cross-correlations (significance level of 0.01) between SSTs and seasonal rainfall showed the influence of SST of Pacific, Indian, and Northern Atlantic Oceans and the Gulf of Guinea on the two seasons of rainfall over the country. In particular, SST regions over the Pacific and northern Atlantic Oceans had a significant teleconnection (remote link) with summer and spring rain peaks at a lead time of 5-6 and 6-7 months, respectively.

学位論文概要

降雨の時空間変動は，人間の活動，特に社会経済的な活動のあらゆる側面に影響を及ぼす。特に，エチオピアの降雨は複雑な地理・地形により，時空間変動が大きいことが特徴として挙げられる。エチオピアの労働力の約 85%を占める農業やエネルギー生産の約 98%を占める水力発電事業にとって，降雨は不可欠であり，エチオピアで最も重要な気象パラメータである。エチオピアの降水量に影響を与える大きな要因の一つは海面水温であり，降水量を予測するための重要な指標となる。エチオピアには，夏の雨季（6～9 月），冬の乾季（10～1 月），春の小雨季（2～5 月）の 3 つの季節があり，これまでのエチオピアの降水量に関する研究のほとんどは夏の雨季のみに焦点を当てており，春季の小雨季に関する研究はほとんど行われていない。そこで，本研究では，春の降雨だけでなく，夏の降雨について局所的・大規模な領域での分析を行い，海面水温とエチオピアの降水量の関係を明らかにすることを目的とする。

第一の研究では，タナ湖流域の夏季降水量データ（1985 年～2015 年）の統計解析を行った。タナ湖は，ナイル川の流量の約 60%を占める青ナイル川の主要な水源である。さらに，海洋の海面水温と夏季降水量との遠隔相関を調査し，人工ニューラルネットワークモデル(ANN)を用いてタナ湖流

域の夏季降水量予測を行った。対象流域の夏季（6 月～9 月）の降雨は単峰的な傾向を示し，7～8 月にピークを持つことがわかった。年間の降水量の変動は，雨季と乾季の間で交互に変動するが，その傾向に大きな変化は見られない。また，有意水準 0.05 での相互相関を調べた結果，雨季の 4～5 ヶ月前の海面水温と夏季降水量の間に有意なテレコネクションがあることが示された。特に，太平洋の 2 つの海面水温域が雨量に影響を与えていることがわかった。さらに，これらの遠隔相関地域を ANN の降水量予測モデルの入力データとして降水量予測を行った。その結果，夏季降水量と海面水温データとの相関係数は 0.8 となり，開発された ANN モデルは流域の降水量予測を行うのに十分な性能を有することが示された。

第二の研究では，海面水温が降水量に及ぼす影響を，流域の局所的な領域（タナ湖流域）からエチオピア全土に拡大して明らかにすることを試みた。さらに，夏季と春季の両雨季を対象とした。分析には，夏季降水量 65 年分と春季降水量 50 年分の長期データが用いられた。その結果，夏季は 7 月～8 月，春季は 4 月～5 月にピークを迎える二峰性の降雨傾向を示すことがわかった。エチオピアでは，地域によって降水パターンが異なるため，いくつかの均質な降雨帯に分割することが重要である。本研究では，エチオピアを 9 つの夏季帯と 5 つの春季帯の 14 の降雨帯に分類した。海面水温

と各降雨帯の季節降水量の相互相関（有意水準 0.01）を行った結果，太平洋，インド洋，北大西洋とギニア湾の海面水温がエチオピアの夏季と春季の降水量に影響を与えることが明らかになった。特に，夏季および春季の降水ピークがそれぞれ 5～6 ヶ月，6～7 ヶ月前の太平洋，インド洋，大西洋北部の海面水温と有意なテレコネクションがあることが明らかになった。

降水量と海水面温度の関係を分析することで，降水量予測の精度が向上することが期待され，本研究で得られた知見は水資源管理，開発計画，洪水・干ばつ対策，エチオピアと下流の隣国（スーダンやエジプト）との水配分計画策定の際に有用である。

List of Publications

1. Alhamshry A, Fenta AA, Yasuda H, Shimizu K, Kawai T (2019) Prediction of summer rainfall over the source region of the Blue Nile by using teleconnections based on sea surface temperatures. Theor. Appl. Climatol 137(3-4), pp: 3077-3087.

   This article mainly covers Chapter 2 of the thesis.

2. Alhamshry A, Fenta AA, Yasuda H, Kimura R, Shimizu K (2020) Seasonal rainfall variability in Ethiopia and its long-term link to global sea surface temperatures. water, 12(1), p.55.

   This article mainly covers Chapter 3 of the thesis.

List of Conferences

1- Alhamshry A, Fenta AA, Yasuda H, Shimizu K, Kawai T (2019). Prediction of summer rainfall over Lake Tana tele connected with global sea surface temperature (oral presentation). International Conference on Water, Informatics, Sustainability, and Environment (August 7-9, 2019). Carlton University, Ottawa, Canada.

2- Alhamshry A, Fenta AA, Yasuda H, Shimizu K, Kawai T (2019). Prediction of summer rainfall over the source region of the Blue Nile (oral presentation). Asia Climate Week (InterMet Asia, InterFlood Asia) (March 26-29, 2019). Suntec City, Singapore.